CALCULATION OF PHONON FREQUENCIES AND WIDTHS IN $Cu_{0.97}A_{0.03}$ ALLOY

CALCULATION OF PHONON FREQUENCIES AND WIDTHS IN $Cu_{0.97}A_{0.03}$ ALLOY

By

DANIEL PATRICK HAMPSON, B.Sc.

A Thesis
Submitted to the School of Graduate Studies
in Partial Filfilment of the Requirements
for the Degree
Master of Science

McMaster University
September 1973

MASTER OF SCIENCE (Physics)
McMASTER UNIVERSITY Hamilton, Ontario

TITLE: Calculation of Phonon Frequencies and Widths in $Cu_{0.97}A_{0.03}$ Alloy

AUTHOR: Daniel Patrick Hampson, B.Sc. (Loyola College)

SUPERVISOR: Professor D. W. Taylor

NUMBER OF PAGES: (vi), 2 + 101

SCOPE AND CONTENTS:

The mean square displacement spectrum of a single mass defect and that of its neighbours is examined for both a light and a heavy defect to observe the extent of the perturbation of the pure crystal.

Nearest neighbour force constant changes for a 3% random distribution of gold defects in a copper host are calculated by fitting to experimental elastic constants for this alloy. The phonon shifts and widths are calculated for the system with various sets of force constant changes, and comparison is made with experiment.

ACKNOWLEDGEMENTS

I would like to thank my supervisor, Dr. Taylor, not only for suggesting the problem, but for enduring most patiently the attempted solution. His timely suggestions have been indispensible in ensuring the progress of the work.

Secondly, I would like to thank my fellow graduate students and colleagues at McMaster for allowing me to play short-stop on the baseball team.

Thirdly, I would like to thank the cleaning staff of McMaster University for not cleaning my notes off the floor.

Finally, I wish to thank Miss Erie Long for doing most of the work that has produced this thesis.

TABLE OF CONTENTS

CHAPTER		PAGE
	INTRODUCTION	A
I	THEORY	1
	1.1 Green's Functions	1
	1.1.1 General Theory	1
	1.1.2 Perfect Crystal Green's Function	8
	1.1.3 Defect Crystal Green's Function	15
	1.2 Solutions of Dyson Equation	19
	1.2.1 Single Mass Defect	21
	1.2.2 Low Concentration Theory	25
	1.2.3 Perturbation Theory	35
	1.3 Neutron Scattering	38
II	CALCULATIONS	44
	2.1 Single Mass Defect	44
	2.2 Copper-Gold Alloy	59
	2.3 Elastic Constants	64
	2.4 Calculation of Shifts and Widths	75
	2.5 Conclusions	88
	APPENDIX I - CRYSTAL SYMMETRY AND PERTURBATION THEORY	90

TABLE OF CONTENTS - continued

CHAPTER PAGE

APPENDIX II - MATRIX ELEMENTS IN THE SYMMETRY DIRECTIONS 97

REFERENCES 100

LIST OF TABLES

TABLE PAGE

1 Mean Square Displacements for $\varepsilon = -2.1$ and $T = 50°K$ 51

2 Mean Square Displacements for $\varepsilon = .575$ and $T = 50°K$ 56

3 $\Delta\omega/\omega$ for $z \to 0$ 66

4 Elastic Constants Measured by O'Hara and Marshall at $T = 300°K$ in Units of 10^{11} dyn/cm^2 68

5 Calculation of Elastic Constant Changes Central Condition: $\Delta 1ZZ = \Delta 1XX - \Delta 1XY$ 71

6 Comparison of Experimental and Calculated Elastic Constant Changes 73

INTRODUCTION

The theory of the effect of a low concentration of defects on the lattice vibrations of a crystal has been worked out by various investigators, including in particular Elliott and Taylor (1964) and Maradudin (1963), who investigated the problem of a single mass defect in a crystal, and later extended the results to include a low concentration of defects based on the multiple scattering of phonons off individual defect sites (Elliott and Taylor (1967)). Theoretical investigations of the phonon shifts and widths were carried out by Lakatos (1967), Lakatos and Krumhansl (1968), and Kesharwani and Agrawal (1971), but no comparison with experiment was done until Bruno and Taylor (1971) calculated the phonon shifts and widths in the T(z00) and T1(zz0) directions in a Cu-Au alloy and compared with the experimental results of Svensson and Kamitakahara (1971). They found that the results could be fitted with nearest neighbour force constant changes, but that the changes required were excessively non-central. Kesharwani and Agrawal (1973) have repeated the calculations using central force constant changes calculated from the Krebs model and have achieved some success in fitting to the experimental results in these directions.

In this thesis the calculations of shifts and widths in the T(zzz) direction for an alloy of 3% gold in Copper will be undertaken using the perturbation technique of Bruno and Taylor (1971). Three constant changes will be determined by fitting to the elastic constants measured by O'Hara and Marshall (1971), and the shifts and widths calculated from these changes as well as those of Bruno and Taylor (1971), and Kesharwani and Agrawal (1973) will be compared with the experimental results of Kamitakahara (1973).

CHAPTER I

THEORY

1.1 Green's Functions

1.1.1 General Theory

The Green's function relevant to the neutron scattering problem is the double-time thermal Green's function of Zubarev (1960). This is defined as follows: if A and B are two operators, then the retarded Green's function $G_r(t,t')$ is:

$$G_r(t,t') = \langle\langle A(t);B(t')\rangle\rangle_r$$

$$= -i\theta(t-t')\langle[A(t),B(t')]\rangle \qquad \text{(I-1)}$$

where $\theta(x)$ is the step function defined by:

$$\theta(x) = \left.\begin{matrix} 1 \\ 0 \end{matrix}\right\} \begin{matrix} x > 0 \\ x < 0 \end{matrix} \quad , \qquad \text{(I-2)}$$

and A(t) is the Heisenberg operator, $A(t) = e^{i\mathcal{H}t/h}Ae^{-i\mathcal{H}t/h}$. $[A(t),B(t')]$ is the commutator for the phonon case, and $\langle A\rangle$ is the thermal average of the operator A. This last is given by

$$\langle A\rangle = \mathrm{Tr}(e^{-\mathcal{H}/kT}A)/\mathrm{Tr}(e^{-\mathcal{H}/kT}) \qquad \text{(I-3)}$$

where $\mathcal{H}$ is the Hamiltonian of the system and T is the temperature. Similarly, the advanced Green's function is:

$$G_a(t,t') = i\theta(t'-t)\langle[A(t),B(t')]\rangle \quad . \qquad \text{(I-4)}$$

The significance of the Green's function lies in its relation to the correlation function $\langle A(t)B(t')\rangle$ which is used in linear response theory to describe the response of the observable A to a probe coupled to the operator B. This relation will be shown below.

The method used to obtain the Green's function is to form an equation of motion based on the equation satisfied by the Heisenberg operators, i.e.,

$$i\hbar\,\frac{dA}{dt} = [A,\mathcal{H}] \quad .$$

Thus, by differentiating $G_r(t,t')$ with respect to t, we get:

$$i\hbar\,\frac{dG}{dt} = \hbar\delta(t-t')\langle[A(t),B(t')]\rangle$$

$$+ \langle\langle[A(t),\mathcal{H}];B(t')\rangle\rangle_r \qquad \text{(I-5)}$$

where use has been made of the fact that

$$\frac{d\theta(t)}{dt} = \delta(t) \quad .$$

The second term on the right represents a basically more complicated object than the original Green's function, and further differentiating generally leads to higher order Green's functions; all of which reflects the difficulties inherent in any general solution of the many-body problem. However, in the particular phonon case, it so happens that this equation of motion can be solved exactly as will be shown below.

Certain general properties of the Green's function are of interest here. First of all, if the Hamiltonian of the many-body system is time independent (as is the case in the phonon problem), then the Green's function depends only on t-t'. This stationarity principle allows us to write:

$$G_r(t,t') = G_r(t-t') = G_r(\tau) \qquad \tau = t-t' \tag{I-6}$$

and similarly

$$G_a(t,t') = G_a(t-t') = G_a(\tau) \quad . \tag{I-7}$$

The relation between the Green's function and the correlation function can be seen explicitly by expressing the Green's function in terms of the so-called spectral representation. This involves choosing a particular set of basis states, namely the eigenfunctions of the full Hamiltonian, $\mathcal{H}$, and expressing the thermal average in terms of these states. The Fourier transform of the Green's function is defined as:

$$G_r(\omega) = \frac{1}{2\pi}\int_{-\infty}^{\infty} G_r(\tau)e^{i\omega\tau}\, d\tau \tag{I-8}$$

$$= \frac{1}{2\pi i}\int_{-\infty}^{\infty} \theta(\tau)\langle A(\tau)B - BA(\tau)\rangle e^{i\omega\tau}\, d\tau \quad . \tag{I-9}$$

In the representation generated by the above mentioned basis states, the correlation function is:

$$\langle A(\tau)B\rangle = \frac{1}{Z}\sum_m \langle m|A(\tau)B|m\rangle e^{-\beta\omega_m} \tag{I-10}$$

where $\beta = \hbar/kT$ and $|m\rangle = Em|m\rangle = \hbar\omega_m|m\rangle$. Using the fact that the set of states, $|m\rangle$, is a complete set, we can write finally:

$$\langle A(\tau)B\rangle = \int_{-\infty}^{\infty} d\omega e^{-i\omega\tau} S(\omega) \tag{I-11}$$

where

$$S(\omega) = \frac{1}{Z}\sum_{mn} e^{-\beta\omega_m} \langle m|A|n\rangle\langle n|B|m\rangle\delta(\omega-\omega_{nm}) \tag{I-12}$$

and

$$\omega_{nm} = \omega_n - \omega_m \quad .$$

$S(\omega)$ is called the spectral function, and depends on both the excitation energies, ω_{nm}, of the Hamiltonian as well as on the operators A and B through the matrix elements, $<m|A|n>$. Furthermore, the spectral function is simply the time Fourier transform of the correlation function in question. Similarly, we can write:

$$<BA(\tau)> = \int_{-\infty}^{\infty} d\omega e^{-i\omega\tau} \tilde{S}(\omega) \tag{I-13}$$

where

$$\tilde{S}(\omega) = \frac{1}{Z} \sum_{mn} e^{-\beta\omega_m} <m|B|n><n|A|m>\delta(\omega+\omega_{\underset{nm}{mn}}) \quad . \tag{I-14}$$

These two spectral functions are related by:

$$\tilde{S}(\omega) = e^{-\beta\omega} S(\omega) \quad , \tag{I-15}$$

which can be seen by simply interchanging the indices m and n in the expression for $\tilde{S}$. In terms of these spectral functions, the Green's function becomes:

$$G_r(\omega) = \frac{1}{2\pi i}\int_{-\infty}^{\infty} \theta(\tau)e^{i\omega\tau}d\tau \int_{-\infty}^{\infty} d\omega' e^{-i\omega'\tau}$$

$$\times\ [1 - e^{-\beta\omega'}]S(\omega') \qquad (I\text{-}16)$$

or, by expressing the step function as:

$$\theta(\tau) = \frac{i}{2\pi}\int_{-\infty}^{\infty} \frac{e^{-ix\tau}}{x+i\varepsilon}\,dx \qquad \varepsilon \to 0^+ \qquad (I\text{-}17)$$

and using the fact that:

$$\delta(x) = \frac{1}{2\pi}\int_{-\infty}^{\infty} dt\ e^{-ixt} \qquad (I\text{-}18)$$

the Green's function becomes finally:

$$G_r(\omega) = \frac{1}{2\pi}\int_{-\infty}^{\infty} d\omega'\ \frac{[1 - e^{-\beta\omega'}]S(\omega')}{\omega - \omega' + i\varepsilon} \qquad (I\text{-}19)$$

$$= \frac{P}{2\pi}\int_{-\infty}^{\infty} d\omega'\ \frac{[1 - e^{-\beta\omega'}]S(\omega')}{\omega - \omega'}$$

$$- \frac{i}{2}\ [1 - e^{-\beta\omega}]S(\omega) \qquad (I\text{-}20)$$

where P denotes the principal value integral. The advanced Green's function has a similar form:

$$G_a(\omega) = \frac{1}{2\pi}\int_{-\infty}^{\infty} \frac{d\omega'[1 - e^{-\beta\omega'}]S(\omega')}{\omega - \omega' - i\varepsilon} \tag{I-21}$$

$$= \frac{P}{2\pi}\int_{-\infty}^{\infty} \frac{d\omega'[1 - e^{-\beta\omega'}]S(\omega')}{\omega - \omega'}$$

$$+ \frac{i}{2}[1 - e^{-\beta\omega}]S(\omega) \quad . \tag{I-22}$$

Several points should be noted here. First of all, the two Green's functions can be considered simply as two branches of the function G(z) defined over the whole complex plane by:

$$G(z) = \frac{1}{2\pi}\int_{-\infty}^{\infty} \frac{d\omega'[1 - e^{-\beta\omega'}]S(\omega')}{z - \omega'} \tag{I-23}$$

where there is presumed to be a cut along the real axis. In this case, the retarded and advanced functions are obtained from G(z) by approaching the real axis from above and below respectively, i.e.,

$$G_r(\omega) = G(\omega + i\varepsilon) \tag{I-24a}$$

$$\varepsilon \to 0^+$$

and $$G_a(\omega) = G(\omega - i\varepsilon) \quad . \tag{I-24b}$$

Secondly, we obtain immediately the desired relation between the Green's function and the correlation function from the spectral representatives. Subtracting Eq. (I-22) from Eq. (I-20) gives:

$$G(\omega + i\varepsilon) - G(\omega - i\varepsilon) = - i[1 - e^{-\beta\omega}]S(\omega) \tag{I-25}$$

or $$2\mathrm{Im}G_r(\omega) = - [1 - e^{-\beta\omega}]S(\omega) \quad . \tag{I-26}$$

Remembering that $S(\omega)$ is, in fact, the Fourier transform of the correlation function, we see that all physical information is contained in the imaginary part of the retarded Green's function and, in fact, the real part is related to the imaginary part as follows:

$$\mathrm{Re}\ G_{r/a}(\omega) = \mp \frac{1}{\pi} P \int_{-\infty}^{\infty} d\omega' \frac{\mathrm{Im}\ G_{r/a}(\omega')}{\omega - \omega'} \tag{I-27}$$

which follows immediately from (I-20). Similarly, the retarded and advanced functions are related by:

$$\mathrm{Re}\ G_r(\omega) = \mathrm{Re}\ G_a(\omega) \tag{I-28a}$$

$$\mathrm{Im}\ G_r(\omega) = - \mathrm{Im}\ G_a(\omega) \quad . \tag{I-28b}$$

1.1.2 Perfect Crystal Green's Function

We consider first the lattice vibrations of a perfect crystal. By "perfect", we mean a crystal consisting of n identical unit cells which has translational symmetry. It is not necessary that all the atoms in the crystal be identical, as for example, a crystal containing more than one atom per unit cell. However, as a consequence of the translational symmetry, it follows that the eigenstates of the perfect crystal Hamiltonian are plane waves. In general, the Hamiltonian for the vibrating crystal is written:

$$= \frac{1}{2} \sum_{\alpha \ell} \frac{p_\alpha^2(\ell)}{2M_\alpha(\ell)} + \frac{1}{2} \sum_{\substack{\alpha\beta \\ \ell\ell'}} A_{\alpha\beta}(\ell\ell') u_\alpha(\ell) u_\beta(\ell') \tag{I-29}$$

where it is assumed that the oscillations of the atoms from their equilibrium positions are small. In the above equation ℓ is the number of the unit cell running from 1 to N, while α and β run over the three cartesian components as well as the several atoms within the unit cell, if the lattice is not a Bravais lattice. It is assumed that each atom oscillates within a potential $\phi\ (\underline{r}_1, \underline{r}_2, \ldots, \underline{r}_N)$, dependent only on the atomic positions, but which may include non-central effects due to the conduction electrons in a metal, etc. Then, if $u_\alpha(\ell)$ is the α-component of the displacement from equilibrium of the ℓ^{th} atom, the coefficients $A_{\alpha\beta}(\ell\ell')$ are simply those of the quadratic term in the Taylor expansion of ϕ about the equilibrium positions, i.e.,

$$A_{\alpha\beta}(\ell\ell') = \left. \frac{\partial^2 \phi}{\partial u_\alpha(\ell)\, \partial u_\beta(\ell')} \right|_0 \quad . \tag{I-30}$$

It is the stipulation of small oscillations which allows us to neglect all other terms in the expansion.

For the neutron scattering problem, the relevant Green's function is the displacement-displacement Green's function:

$$G_{\alpha\beta}(\ell\ell';\tau)_{r/a} = \frac{2\pi}{\hbar} <<u_{\alpha}(\ell,\tau);u_{\beta}(\ell';0)>>_{r/a} \quad . \tag{I-31}$$

Using this function and the Hamiltonian (I-29), the equation of motion (I-5) becomes:

$$i\hbar \frac{d}{d\tau} G_{\alpha\beta}(\ell\ell';\tau) = 2\pi\delta(\tau)<[u_{\alpha}(\ell,\tau),u_{\beta}(\ell',0)]> + \frac{2\pi}{\hbar} <<[u_{\alpha}(\ell,\tau),\mathcal{H}];u_{\beta}(\ell',0)>> \tag{I-32}$$

or:

$$\frac{d}{d\tau} G_{\alpha\beta}(\ell\ell';\tau) = \frac{2\pi}{\hbar}\frac{1}{M_{\alpha}(\ell)} <<p_{\alpha}(\ell,\tau);u_{\beta}(\ell',0)>> \quad . \tag{I-33}$$

A second differentiation with respect to τ gives:

$$i\hbar \frac{d^2}{d\tau^2} G_{\alpha\beta}(\ell\ell';\tau) = \frac{2\pi}{M_{\alpha}(\ell)} \delta(\tau)<[p_{\alpha}(\ell,\tau);u_{\beta}(\ell',0)]> + \frac{2\pi}{\hbar M_{\alpha}(\ell)} <<[p_{\alpha}(\ell,\tau),\mathcal{H}];u_{\beta}(\ell';0)>> \tag{I-34}$$

and finally an equation consisting entirely of the Green's function:

$$- M_\alpha(\ell) \frac{d^2}{d\tau^2} G_{\alpha\beta}(\ell\ell';\tau) = 2\pi\delta(\tau)\delta(\ell\ell')\delta(\alpha,\beta) + \sum_{\substack{\gamma \\ \ell''}} A_{\alpha\gamma}(\ell\ell'')G_{\gamma\beta}(\ell'',\ell';\tau) \ . \tag{I-35}$$

It is convenient at this point to use the Fourier transformed Green's function:

$$G_{\alpha\beta}(\ell\ell';\tau) = \int_{-\infty}^{\infty} d\omega e^{-i\omega\tau} G_{\alpha\beta}(\ell\ell';\omega) \tag{I-36}$$

and secondly, to define the mass reduced quantities:

$$g_{\alpha\beta}(\ell\ell';\omega) = \sqrt{M_\alpha(\ell)M_\beta(\ell')} \ G_{\alpha\beta}(\ell\ell';\omega) \tag{I-37a}$$

$$a_{\alpha\beta}(\ell\ell') = \frac{A_{\alpha\beta}(\ell\ell')}{\sqrt{M_\alpha(\ell)M_\beta(\ell')}} \ . \tag{I-37b}$$

Equation (I-35) then becomes:

$$\omega^2 g_{\alpha\beta}(\ell\ell';\omega) = \delta(\ell\ell')\delta(\alpha,\beta) + \sum_{\substack{\gamma \\ \ell''}} a_{\alpha\gamma}(\ell\ell'') \times g_{\gamma\beta}(\ell'',\ell';\omega) \ . \tag{I-38}$$

Up to this point, the assumption of a "perfect" crystal has not been used, i.e., the masses of the atoms have been allowed to vary from one position to another and no stipulation has been made concerning the force constants $A_{\alpha\beta}(\ell\ell')$. Therefore, Eq. (I-38) is completely general and will be used below to derive the defect-crystal Green's function. To solve for the case of the perfect crystal, it is convenient to transform to the so-called "normal coordinates" by means of the unitary matrix defined by:

$$U(jk;\alpha\ell) = N^{-1} \sigma_\alpha^j(\underline{k})\exp(i\underline{k}\cdot\underline{R}_\ell) \qquad \text{(I-39)}$$

where $\sigma_\alpha^j(\underline{k})$ is the eigenvector of the dynamical matrix associated with the force constant matrix:

$$D_{\alpha\beta}(\underline{k}) = \sum_{\ell\ell'} a_{\alpha\beta}(\ell-\ell')\exp[i\underline{k}\cdot(\underline{R}_\ell - \underline{R}_{\ell'})] \qquad \text{(I-40)}$$

and $\underline{R}_\ell$ is the position of the ℓ^{th} unit cell. It follows from the translational symmetry of the perfect crystal that $a_{\alpha\beta}(\ell\ell')$ depends only on the distance between the unit cells:

$$a_{\alpha\beta}(\ell,\ell') = a_{\alpha\beta}(\ell-\ell') \quad . \qquad \text{(I-41)}$$

Then the $\sigma_\alpha^j(\underline{k})$ satisfy the eigenvalue problem:

$$\sum_\beta D_{\alpha\beta}(\underline{k})\sigma_\beta^j(\underline{k}) = \omega_j^2(\underline{k})\sigma_\alpha^j(\underline{k}) \quad . \qquad \text{(I-42)}$$

It is assumed throughout the following that a Bravais lattice is being considered. Then j numbers the three eigenvalues of the above equation. Finally, since the eigenvectors can be chosen to satisfy the relations:

$$\sum_{\alpha} \sigma_{\alpha}^{*j}(\underline{k})\sigma_{\alpha}^{j'}(\underline{k}) = \delta_{jj'} \tag{I-43a}$$

and

$$\sum_{j} \sigma_{\alpha}^{*j}(\underline{k})\sigma_{\beta}^{j}(\underline{k}) = \delta_{\alpha\beta} \tag{I-43b}$$

(Maradudin, Montroll and Weiss (1963)) it can be seen that U is the matrix which diagonalizes the matrix a:

$$\sum_{\substack{\alpha\beta \\ \ell\ell'}} U(j\underline{k};\alpha\ell)a_{\alpha\beta}(\ell\ell')U^*(j'\underline{k}';\beta\ell') = \delta_{jj'}\delta_{kk'}\omega_j^2(\underline{k}) \tag{I-44}$$

where $\underline{k}$ and $\underline{k}'$ run over the N values within the first Brillouin zone, and j, j' run over the three branches corresponding to the eigenvalues of (I-42). That the matrix U is unitary follows from the relation:

$$\sum_{\ell} \exp[i\underline{k}\cdot\underline{R}_{\ell}] = N\Delta(\underline{k}) \tag{I-45}$$

where $\Delta(\underline{k}) = 0$ unless $\underline{k}$ is a reciprocal lattice vector. Thus, if Eq. (I-38) is written in matrix form:

$$\omega^2 g = I + ag \qquad \text{(I-46)}$$

then the transformed equation becomes:

$$\omega^2 UgU^+ = I + UaU^+UgU^+ \qquad \text{(I-47)}$$

or $$\omega^2 \tilde{g} = I + \tilde{a}\tilde{g} \quad . \qquad \text{(I-48)}$$

In the case of the perfect crystal, we know from Eq. (I-44) that

$$\tilde{a}(jj';kk') = \delta_{jj'}\delta_{kk'}\omega_j^2(\underline{k}) \quad . \qquad \text{(I-49)}$$

So the equation reduces to:

$$\omega^2 \tilde{p}(jj';kk') = \delta_{jj'}\delta_{kk'} + \omega_j^2(\underline{k})\tilde{p}(jj';kk') \qquad \text{(I-50)}$$

where the perfect crystal Green's function is written as $\tilde{p}$. This equation may be solved to give:

$$\tilde{p}(jj';kk') = \frac{\delta_{jj'}\delta_{kk'}}{\omega^2 - \omega_j^2(\underline{k})} \qquad \text{(I-51)}$$

showing that the perfect crystal Green's function is diagonal in normal coordinate space, as expected. Finally, by performing the inverse transformation, the Green's function in real space is:

$$p = U^{+}\,\tilde{p}\,U \tag{I-52}$$

or:

$$p_{\alpha\beta}(\ell\ell';\omega) = \frac{1}{N}\sum_{jk} \frac{\sigma_{\alpha}^{*j}(\underline{k})\,\sigma_{\beta}^{j}(\underline{k})\,e^{-i\underline{k}\cdot(\underline{R}_{\ell}-\underline{R}_{\ell'})}}{\omega^{2} - \omega_{j}^{2}(\underline{k})} \; . \tag{I-53}$$

1.1.3 Defect Crystal Green's Function

The defect crystal is one in which certain atoms of the perfect crystal are replaced by atoms of a different mass and possibly a chemically different species. The more numerous atoms are called the host, and the others are called the impurity or defect. No assumption is made at this point concerning changes in the relative positions of the host or defect atoms, as a result of the substitution. However, these changes will become relevant in applying the formalism to the study of the neutron-scattering problem as will be seen below.

If the mass of the host atom is M, then the change in the mass of the atom at site ℓ as a result of the impurity substitution is conveniently written in terms of the parameter $\varepsilon(\ell)$ as:

$$M(\ell) - M = -\varepsilon(\ell)M \quad , \tag{I-54}$$

(where Bravais lattice is assumed). Similarly, the force constants $B_{\alpha\beta}(\ell\ell')$ of the defect crystal are written:

$$B_{\alpha\beta}(\ell\ell') = A_{\alpha\beta}(\ell\ell') + \Delta A_{\alpha\beta}(\ell\ell') \tag{I-55}$$

where $A_{\alpha\beta}(\ell\ell')$ are the force constants between the host atoms in the perfect crystal. It should be observed that the force constants between host atoms of the defect crystal may be changed due to the deformation of the crystal about an impurity. In general, the matrix ΔA has non-zero elements clustered on and about the defect sites and this set of sites around a given defect is called the "defect space".

With these definitions, the equation for the defect crystal Green's function may be obtained, using Eq. (I-38) in the form:

$$M(\ell)\omega^2 G_{\alpha\beta}(\ell\ell';\omega) = \delta(\ell\ell')\delta(\alpha\beta) + \sum_{\substack{\gamma \\ \ell''}} B_{\alpha\gamma}(\ell\ell'')G_{\gamma\beta}(\ell'',\ell';\omega) \tag{I-56}$$

or, using (I-54) and (I-55),

$$[1 - \varepsilon(\ell)]M\omega^2 G_{\alpha\beta}(\ell\ell';\omega) = \delta(\ell\ell')\delta(\alpha\beta) + \sum_{\substack{\gamma \\ \ell''}} A_{\alpha\gamma}(\ell\ell'')G_{\gamma\beta}(\ell'',\ell';\omega) + \sum_{\substack{\gamma \\ \ell''}} \Delta A_{\alpha\gamma}(\ell\ell'')G_{\gamma\beta}(\ell'',\ell';\omega) \quad . \tag{I-57}$$

Introducing the defect matrix:

$$C_{\alpha\beta}(\ell\ell';\omega) = \delta(\ell\ell')\delta_{\alpha\beta}M\varepsilon(\ell)\omega^2 + \Delta A_{\alpha\beta}(\ell\ell') \tag{I-58}$$

and reverting to the mass-reduced quantities:

$$g = MG \quad \text{and} \quad a = \frac{A}{M} \quad , \quad c = \frac{C}{M} \tag{I-59}$$

we get the equation in matrix notation:

$$\omega^2 g = I + ag + cg \quad . \tag{I-60}$$

But if p is the perfect crystal Green's function, it must satisfy

$$\omega^2 p = I + ap \tag{I-61}$$

or

$$p = (\omega^2 I - a)^{-1} \quad . \tag{I-62}$$

Then Eq. (I-60) becomes finally:

$$g = p + pcg \qquad \text{(I-63)}$$

which is in the form of a Dyson equation for g.

1.2 Solutions of Dyson Equation

The starting point for the defect problem is the Dyson equation (I-63):

$$G = P + PVG \quad . \tag{I-64}$$

The solution of the problem depends on the precise nature of the matrix V, which is given by Eq. (I-58):

$$V_{\alpha\beta}(\ell\ell') = \Delta\Phi_{\alpha\beta}(\ell\ell') + M\varepsilon(\ell)\omega^2 \, \delta_{\alpha\beta}\delta(\ell\ell') \quad . \tag{I-65}$$

In general, this matrix of dimension 3N×3N, consists of a series of blocks down the diagonal with zeros at other points. There is one block for each defect centred at the defect site and the size of the block corresponds to the "defect space" defined above. As is obvious from Eq. (I-65), it is the force constant changes which cause the off-diagonal disorder, i.e., off-diagonal non-zero elements of V, and because of this, the possibility exists of overlapping blocks. Furthermore, the precise nature of V depends on the configuration of defects in the crystal. Since this is generally unknown, a configurational average must be performed, in the same way that unknown variables are averaged in statistical mechanics.

1.2 Solutions of Dyson Equation

The starting point for the defect problem is the Dyson equation (I-63):

$$G = P + PVG \quad . \tag{I-64}$$

The solution of the problem depends on the precise nature of the matrix V, which is given by Eq. (I-58):

$$V_{\alpha\beta}(\ell\ell') = \Delta\Phi_{\alpha\beta}(\ell\ell') + M\varepsilon(\ell)\omega^2 \, \delta_{\alpha\beta}\delta(\ell\ell') \quad . \tag{I-65}$$

In general, this matrix of dimension 3N×3N, consists of a series of blocks down the diagonal with zeros at other points. There is one block for each defect centred at the defect site and the size of the block corresponds to the "defect space" defined above. As is obvious from Eq. (I-65), it is the force constant changes which cause the off-diagonal disorder, i.e., off-diagonal non-zero elements of V, and because of this, the possibility exists of overlapping blocks. Furthermore, the precise nature of V depends on the configuration of defects in the crystal. Since this is generally unknown, a configurational average must be performed, in the same way that unknown variables are averaged in statistical mechanics.

Several special cases are of interest: First, the single mass-defect; this corresponds to replacing a single host atom by another atom of different mass, such that the force constants throughout the crystal remain unchanged. Although this is obviously an artificial problem, it is important for several reasons: (a) the single defect is the only problem which can be solved exactly and shows the general nature of phonon scattering off defects; (b) it is believed that the mass changes account for most of the phonon scattering, while the force constant changes produce secondary corrections; and (c) the scattering of phonons off low concentrations of defects can be approximated by multiple scattering off single defects, thus involving the t-matrix for single defect scattering.

The second case is that of a low concentration of mass defects situated randomly throughout the crystal. The random configuration ensures that the averaging will restore the translational symmetry of the crystal, while the low concentration ensures that coherent scattering off groups of defects will be negligible and only the single defect scattering described above need be considered.

Finally, we will consider the case of a low concentration of defects with force constant changes, under the assumption that the concentration of defects is sufficiently low and the defect spaces sufficiently small that the probability of two defect spaces overlapping is taken to be zero. Under these assumptions, this problem is essentially the same as the mass defect problem above, while the increased difficulty is due to the short-ranged off-diagonal disorder.

1.2.1 Single Mass Defect

Equation (I-64) is easy to solve for the case of a single mass defect at the origin. The V-matrix can then be written:

$$V_{\alpha\beta}(\ell\ell') = M\varepsilon\omega^2 \, \delta_{\alpha\beta}\delta(\ell\ell')\delta(\ell 0) \quad . \tag{I-66}$$

Equation (I-64) then becomes:

$$G_{\alpha\beta}(\ell\ell') = P_{\alpha\beta}(\ell\ell') + \sum_{\gamma} P_{\alpha\gamma}(\ell 0)M\varepsilon\omega^2 \, G_{\gamma\beta}(0\ell') \quad . \tag{I-67}$$

It is well known (Maradudin et al. (1963)) that the Green's function for the perfect crystal must transform under the operations of the crystal point group in the same way as the force constant matrix, i.e., if $S_{\alpha\beta}$ represents an operation of the group, then:

$$P_{\alpha\beta}(LL') = \sum_{\gamma\delta} S_{\alpha\gamma}P_{\gamma\delta}(\ell\ell')S_{\beta\delta} \tag{I-68}$$

where the operation S takes the atom at ℓ' into the new position L' and the atom at ℓ into the position L. By applying Eq. (I-68) to those elements of the crystal group which leave certain atoms unmoved, various relationships among the elements of the P-matrix may be deduced. This is shown more explicitly for the F.C.C. case in Appendix I. Here, it is sufficient to note that for the case of cubic crystals, the following result can be shown: (Taylor (1964))

$$P_{\alpha\beta}(\ell\ell;\omega) = P_{\alpha\beta}(00;\omega) = \delta_{\alpha\beta}P(0;\omega) \quad . \qquad \text{(I-69)}$$

Equation (I-67) can then be solved to yield the Green's function for the single mass-defect case:

$$G_{\alpha\beta}(\ell\ell') = P_{\alpha\beta}(\ell\ell') + \sum_{\gamma} \frac{P_{\alpha\gamma}(\ell 0)M\varepsilon\omega^2 P_{\gamma\beta}(0\ell')}{1 - M\varepsilon\omega^2 P(0;\omega)} \quad . \qquad \text{(I-70)}$$

In particular, the defect-defect Green's function becomes:

$$G_{\alpha\beta}(00\overset{w}{\underset{\wedge}{}}) = \frac{P(0;\omega)}{1 - M\varepsilon\omega^2 P(0;\omega)}\,\delta_{\alpha\beta} \quad . \qquad \text{(I-71)}$$

From Eq. (I-70), we can see that the quantity

$$\frac{M\varepsilon\omega^2}{1 - M\varepsilon\omega^2 P(0;\omega)}$$

is the single-defect scattering t-matrix referred to above (Klein (1963)).

We will be considering correlation functions like:

$$<u^2> = 3<u_\alpha(\ell,\tau=0)u_\alpha(\ell)> \tag{I-72}$$

$$= -\frac{3\hbar}{2\pi}\int_{-\infty}^{\infty}\frac{d\omega}{e^{\beta\omega}-1}\{2\mathrm{Im}\,G^R_{\alpha\alpha}(\ell\ell;\omega)\} \tag{I-73}$$

where $<u^2>$ is the mean square displacement of the atom at position ℓ from equilibrium. The last equation follows from the relation (I-11) between the correlation function and the spectral function, along with Eq. (I-26) relating the spectral function and the imaginary part of the Green's function.

At the defect site, the displacement spectrum $<u^2(\omega)>$ is proportional to

$$\mathrm{Im}G^R_{\alpha\alpha}(0;\omega) = \frac{\mathrm{ImP}(0;\omega)}{[(1-M\varepsilon\omega^2\mathrm{ReP}(0;\omega)]^2 + [M\varepsilon\omega^2\mathrm{ImP}(0;\omega)]^2} \tag{I-74}$$

showing a resonance at that value of $\omega = \omega_R$ satisfying:

$$1 - M\varepsilon\omega_R^2\mathrm{ReP}(0;\omega_R) = 0 \tag{I-75}$$

with a half-width at half-maximum given by

$$M\varepsilon\omega_R^2\mathrm{ImP}(0;\omega_R) \tag{I-76}$$

if ω_R is contained within the range in which the density of states of the perfect crystal is non-zero. It can be shown that ω_R is within this range only if the defect is heavier than the host atoms, i.e., $\varepsilon < 0$ (Taylor (1964)). Then ω_R can be thought of as the frequency at which the defect naturally tends to resonate, while the finite width is due to the decay of the mode into the nearby perfect crystal modes. In fact, for the case of a light defect ($0 < \varepsilon < 1$), the value of ω satisfying (I-75) may be outside the perfect crystal band. In this range the imaginary part of P, which is proportional to the density of states, vanishes, so that ImG contributes a pole to the integral (I-73). This mode is called a "local mode" as it can be shown that the spatial extent of this vibration decays exponentially with distance from the defect.

For the atoms neighbouring the defect, the displacement spectrum $\langle u^2(\omega)\rangle$ is proportional to:

$$\mathrm{Im}G^R_{\alpha\alpha}(\ell\ell;\omega) = \mathrm{Im}\{P(0;\omega) + \sum_{\gamma} P_{\alpha\gamma}(\ell 0)\,\frac{M\varepsilon\omega^2}{1 - M\varepsilon\omega^2 P(0;\omega)}\,P_{\gamma\alpha}(0\ell)\} \; . \tag{I-77}$$

This equals ImP(0) plus a correction term due to the presence of the defect which contains the resonance denominator multiplied by $P(0\ell)^2$. This can be expected to get smaller as ℓ gets larger, since $P(0\ell)$ measures the correlation between atoms 0 and ℓ.

Thus the main feature of the heavy-defect spectrum is the resonance which predominates at the defect site and becomes less important for increasingly distant neighbours.

1.2.2 Low Concentration Theory

The aim of the low concentration theory is to solve the Dyson equation to the first order in the concentration, c. As outlined above, the underlying assumptions are:

(a) defects are randomly situated throughout the lattice, so that the probability of finding a defect at any given site is equal to the concentration c.

(b) effects due to the overlapping of defect spaces or the coherent scattering of phonons off pairs or other clusters of defects, enter as second and higher order corrections in the concentration and may be neglected.

Several approaches have been used to arrive at the low concentration result. In particular, the diagrammatic analysis outlined by Langer (1961) for the one-dimensional lattice and subsequently extended by other investigators (e.g., Maradudin (1963), Aiyer et al. (1969)) has the advantage that higher order corrections can be included in a fairly straightforward way. However, it is convenient for this analysis to outline the algebraic approach of Taylor (1967).

Since the defect spaces do not overlap, we can write the matrix as:

$$V = \sum_n V^n \tag{I-78}$$

where V^n is the contribution from the defect at the n^{th} crystal site. In principal, the summation is over all sites but the matrix V^n vanishes if the site n does not contain a defect. A non-zero V^n consists of a single block centred on the n^{th} position on the diagonal, and may be written:

$$V^n_{\alpha\beta}(\ell\ell';\omega) = \Delta\Phi^n_{\alpha\beta}(\ell\ell') + M\varepsilon(n)\omega^2\delta(\ell\ell')\delta_{\alpha\beta} \quad . \tag{I-79}$$

The Dyson equation becomes:

$$G = P + \sum_n PV^nG \quad . \tag{I-80}$$

It is convenient to separate out the scattering due to the impurity at n by writing:

$$G - PV^nG = (I - PV^n)G \equiv G^n \tag{I-81}$$

where, obviously:

$$G^n = P + \sum_{m\neq n} PV^m G \quad . \qquad \text{(I-82)}$$

Thus G^n is the Green's function representing the scattering of phonons off all the defects except that at n. From (I-81), the final Green's function is:

$$G = (I - PV^n)^{-1} G^n \qquad \text{(I-83)}$$

so that (I-80) becomes:

$$G = P + \sum_{n} PV^n (I - PV^n)^{-1} G^n \qquad \text{(I-84a)}$$

and: $$G^n = P + \sum_{m\neq n} PV^m (I - PV^m)^{-1} G^m \quad . \qquad \text{(I-84b)}$$

We can now define the T-matrix, T^n, by:

$$T^n = V^n (I - PV^n)^{-1} \quad . \qquad \text{(I-85)}$$

T^n is a matrix of dimension 3N×3N, with a single block on the diagonal at the nth site if there is a defect at n, and equals zero otherwise. To see that T^n is the usual t-matrix for the scattering of phonons from a single defect, it is sufficient to assume that $V^m = 0$ for all $m\neq n$, and then Eq. (I-84a) becomes:

$$G = P + PT^nP \quad . \tag{I-86}$$

In terms of the t-matrix, the Eqs. (I-84a) and (I-84b) become:

$$G = P + \sum_n PT^nG^n \tag{I-87a}$$

and $$G^n = P + \sum_{m\neq n} PT^mG^m \quad . \tag{I-87b}$$

It is now necessary to do a configuration averaging. For this purpose, it is assumed that all defects are identical. Then, since P is independent of the configuration of defects, it is necessary to evaluate terms like

$$\langle T^nG^n \rangle = \frac{1}{N_c} \Sigma T^nG^n \tag{I-88}$$

where the sum is over all configurations and N_c is the number of possible configurations consistent with the given concentration. Since T^n vanishes for all configurations which do not have a defect at n, it follows that:

$$\langle T^nG^n \rangle = ct^n \langle G^n \rangle_n \tag{I-89}$$

where t^n is identical with T^n, except that it is independent of the configuration, i.e., it assumes there <u>is</u> a defect at n. $\langle G^n \rangle_n$ is the average over all configurations subject to the condition that a defect exists at n. The fact that all defects are identical ensures that t^n is a matrix consisting of a single block centred at n, and that the only dependence on n is the position of this block.

Finally, Eqs. (I-87a) and (I-87b) become:

$$\langle G\rangle = P + \sum_n Pct^n \langle G^n\rangle_n \tag{I-90a}$$

and $$\langle G^n\rangle_n = P + \sum_{m\neq n} Pct^m \langle G^m\rangle_{m,n} \quad . \tag{I-90b}$$

Here, the quantity $\langle G^m\rangle_{m,n}$ is the Green's function averaged over all configurations subject to the condition that a defect exists at positions m <u>and</u> n. Obviously the quantity $\langle G^m\rangle_{m,n} - \langle G^m\rangle_m$ is related to the correlation between the defects at m and n. Taking this latter quantity to be zero is equivalent to the assumption that the phonon scattering at the site m is independent of where the other defects are, i.e., the scattering off the several sites is incoherent. This assumption was pointed out at the beginning of this section, and is now seen to be necessary in order to solve the Eqs. (I-90a) and (I-90b). Any quantity which depends on the positions of two defects must be proportional to c^2 after the averaging procedure. Hence, by setting

$$\langle G^m\rangle_{m,n} = \langle G^m\rangle_m \quad ,$$

we are neglecting terms of second and higher orders in c. The equations become:

$$\langle G\rangle = P + c\sum_n Pt^n\langle G^n\rangle_n \qquad \text{(I-91a)}$$

$$\langle G^n\rangle_n = P + c\sum_{m\neq n} Pt^m\langle G^m\rangle_m \quad . \qquad \text{(I-91b)}$$

Switching indices in (I-91b) and substracting (I-91b) from (I-91a) gives:

$$\langle G\rangle - \langle G^m\rangle_m = cPt^m\langle G^m\rangle_m \qquad \text{(I-92)}$$

or: $$\langle G^m\rangle_m = (I + cPt^m)^{-1}\langle G\rangle \quad . \qquad \text{(I-93)}$$

Finally plugging this result into (I-91a), we get:

$$\langle G\rangle = P + c\sum_n Pt^n(I + cPt^n)^{-1}\langle G\rangle \qquad \text{(I-94)}$$

$$= P + c\sum_n Pv^n(I - (1-c)Pv^n)^{-1}\langle G\rangle \qquad \text{(I-95)}$$

where v^n is defined in analogy with t^n, i.e., for every n, v^n consists of an identical block centred on the diagonal at the position n. Since the summation is over all crystal sites, it can be seen that the quantity:

$$X = \sum_n v^n(I - (1-c)Pv^n)^{-1} \qquad \text{(I-96)}$$

has the same translational symmetry as the perfect crystal, i.e.:

$$X_{\alpha\beta}(\ell\ell') = X_{\alpha\beta}(\ell - \ell') \tag{I-97}$$

a property which will be used in the neutron scattering problem below.

The Dyson equation in this form:

$$\langle G\rangle = P + cPX\langle G\rangle \tag{I-98}$$

can be transformed to normal coordinates using the transformation (I-39). Since X has the translational symmetry of the perfect crystal, it follows that the transformed quantity is diagonal in $\underline{k}$. We can write:

$$\Sigma(\omega) = cUX(\omega)U^{+} \tag{I-99}$$

or explicitly

$$\Sigma^{jj'}(\underline{k},\omega) = c \sum_{\substack{\ell\ell' \\ \alpha\beta}} U(j\underline{k};\alpha\ell)X_{\alpha\beta}(\ell\ell')U^{*}(j'\underline{k};\beta\ell') \tag{I-100}$$

giving for the Dyson equation:

$$G^{jj'}(\underline{k},\omega) = \delta_{jj'}P^{j}(\underline{k},\omega) + \sum_{j'} P^{j}(\underline{k},\omega)\Sigma^{jj'}(\underline{k},\omega)G^{jj'}(\underline{k},\omega) \ . \tag{I-101}$$

If $\underline{k}$ is in a symmetry direction, it can be shown (Appendix II) that $\Sigma^{jj'}(\underline{k},\omega)$ is diagonal in j. Then the equation can be solved immediately to give:

$$G^{j}(\underline{k},\omega) = [\omega^2 - \omega_j^2(\underline{k}) - \Sigma^{j}(\underline{k},\omega)]^{-1} \tag{I-102}$$

where use has been made of the fact that:

$$P^{j}(\underline{k},\omega) = [\omega^2 - \omega_j^2(\underline{k})]^{-1} \quad . \tag{I-103}$$

Thus the quantity Σ appears as a phonon self-energy due to the scattering of phonons off the defects. The defect crystal phonons have energies shifted from the perfect crystal ones by an amount

$$\approx \frac{\mathrm{Re}\Sigma^{j}(\underline{k},\omega_j(\underline{k}))}{2\omega_j(\underline{k})}$$

with a finite lifetime related to

$$\frac{\mathrm{Im}\Sigma^{j}(\underline{k},\omega_j(\underline{k}))}{2\omega_j(\underline{k})} \quad .$$

These results will be used in the neutron scattering problem below.

The self-energy can be evaluated most readily for the case of a low concentration of mass-defects, since the defect matrix v^n is diagonal. In fact,

$$v^{n}_{\alpha\beta}(\ell\ell') = M\varepsilon\omega^{2}\delta(\ell\ell')\delta_{\alpha\beta}\delta(\ell,n) \quad . \tag{I-104}$$

The self-energy in coordinate space is given by Eq. (I-96):

$$X_{\alpha\beta}(\ell\ell') = \sum_{n}\sum_{\gamma\ell''} v^{n}_{\alpha\gamma}(\ell\ell'')Y^{n}_{\gamma\beta}(\ell''\ell') \tag{I-105}$$

where

$$Y^{n} = [I - (1-c)Pv^{n}]^{-1} \quad . \tag{I-106}$$

To evaluate Y^{n}, we note that by definition of the inverse it must satisfy:

$$Y^{n} - (1-c)Pv^{n}Y^{n} = I \tag{I-107}$$

or using the definition (I-104) for v^{n}

$$Y^{n}_{\alpha\beta}(\ell\ell') = (1-c)M\varepsilon\omega^{2}\sum_{\gamma} P_{\alpha\gamma}(\ell n)Y^{n}_{\gamma\beta}(n\ell') + \delta_{\alpha\beta}\delta(\ell\ell') \quad . \tag{I-108}$$

But, if we make the replacement ℓ=n in the above equation and use the cubic crystal result

$$P_{\alpha\beta}(nn) = P_{\alpha\beta}(00) = \delta_{\alpha\beta}P(0;\omega)$$

we get:

$$Y^{n}_{\gamma\beta}(n\ell') = (1-c)M\varepsilon\omega^{2}P(0;\omega)Y^{n}_{\gamma\beta}(n\ell') + \delta_{\alpha\beta}\delta(n\ell') \quad . \tag{I-109}$$

This can be solved to give:

$$Y^{n}_{\gamma\beta}(n\ell') = \frac{\delta_{\gamma\beta}\delta(n\ell')}{1-(1-c)M\varepsilon\omega^{2}P(0;\omega)} \quad . \tag{I-110}$$

So that Eq. (I-108) becomes finally:

$$Y^{n}_{\alpha\beta}(\ell\ell') = \frac{(1-c)M\varepsilon\omega^{2}P_{\alpha\beta}(\ell n)\delta(n\ell')}{1-(1-c)M\varepsilon\omega^{2}P(0;\omega)} + \delta_{\alpha\beta}\delta(\ell\ell') \quad . \tag{I-111}$$

Inserting this result into (I-105) and using the definition (I-104) for v^{n} gives after some rearrangement:

$$\begin{aligned} X_{\alpha\beta}(\ell\ell') &= \sum_{n} \frac{M\varepsilon\omega^{2}}{1-(1-c)M\varepsilon\omega^{2}P(0;\omega)}\,\delta_{\alpha\beta}\delta(\ell\ell')\delta(\ell n) \\ &= \frac{M\varepsilon\omega^{2}}{1-(1-c)M\varepsilon\omega^{2}P(0;\omega)}\,\delta_{\alpha\beta}\delta(\ell\ell') \quad . \end{aligned} \tag{I-112}$$

We see that for the case of the low concentration of mass defects, the X-matrix is diagonal and has the translational symmetry of the perfect crystal. Furthermore, the fact that it is proportional to the identity matrix means that the self-energy Σ as calculated by Eq. (I-100) is independent of both j and $\underline{k}$, and is given by:

$$\Sigma^{jj'}(\underline{k},\omega) = \frac{c\,M\varepsilon\omega^{2}}{1-(1-c)M\varepsilon\omega^{2}P(0;\omega)}\,\delta_{jj'} \quad . \tag{I-113}$$

That the self-energy is independent of both the branch and the wave-vector reflects the fact that the defect has no spatial extent, i.e., isotropic.

1.2.3 Perturbation Theory

When the low concentration of defects includes force constant changes, the problem is much more difficult to solve. For example, in the case of an F.C.C. lattice with only nearest neighbour force constant changes, the defect space has dimensions 39×39. Evaluating the X-matrix by Eq. (I-96) is facilitated by transforming to symmetry coordinates which block diagonalize the matrices (Lakatos and Krumhansl (1969)). However, a further approximation is possible which eliminates the necessity of inverting matrices and hence greatly reduces the calculations involved. This procedure assumes that the defect matrix v^n may be split into two parts:

$$v^n = v_0^n + v_p^n \qquad \text{(I-114)}$$

where it is assumed that the X-matrix corresponding to v_0^n can be calculated exactly:

$$X_0^n = v_0^n[I - (1-c)Pv_0^n]^{-1} \quad . \qquad \text{(I-115)}$$

It is obvious from the preceding section that this will be the case if v_0^n includes mass changes only. Furthermore, it is assumed that v_p^n can be considered a small perturbation whose effect need be included to first order only. If v_p^n is taken to include the force constant changes, then since $v_0^n = M\varepsilon\omega^2 I$, it would appear that this last condition is not satisfied for low ω. This point will be discussed later.

Equation (I-115) can be inverted immediately to give:

$$v_0^n = [I + (1-c)X_0^n P]^{-1} X_0^n \quad . \tag{I-116}$$

Inserting (I-114) and (I-116) into Eq. (I-96) gives:

$$X^n\{I - (1-c)P[(I + (1-c)X_0^n P]^{-1} X_0^n + v_p^n]\}$$
$$= \{[I + (1-c)X_0^n P]^{-1} X_0^n + v_p^n\} \quad . \tag{I-117}$$

This can be manipulated to give:

$$X^n[I - (1-c)Pv_p^n(I + (1-c)PX_0^n)]$$
$$= v_p^n[I + (1-c)PX_0^n] + X_0^n \quad . \tag{I-118}$$

Assuming that v_p^n is a small perturbation allows us to write to first order in v_p^n:

$$X^n \simeq [X_0^n + v_p^n(I + (1-c)PX_0^n][I + (1-c)Pv_p^n(I + (1-c)PX_0^n)] \tag{I-119}$$

$$\simeq X_0^n + v_p^n + (1-c)v_p^nPX_0^n + (1-c)X_0^nPv_p^n$$

$$+ (1-c)^2\, X_0^nPv_p^nPX_0^n \quad . \tag{I-120}$$

The simplification introduced is obvious since the first and fifth terms have entries only on the diagonal of the defect site, while the third and fourth terms are simply column and row matrices connecting to the defect site. Furthermore, the necessity of inverting matrices has been eliminated.

1.3 Neutron Scattering

The low concentration theory can be used to solve the problem of the scattering of thermal neutrons from crystals with low concentrations of defects. The formalism relating the neutron scattering cross section to the defect crystal Green's functions is well known (Lakatos (1967)) and it is sufficient here to present the results for the coherent inelastic scattering which is the concern of this thesis.

If the crystal is bombarded with low-energy neutrons, they may be considered a weak time-dependent perturbation of the crystal system and the differential cross section for the scattering of neutrons through solid angle $d\Omega$ with energy change E is given by Fermi's golden rule:

$$\frac{d^2\sigma}{d\Omega dE} = \frac{k'}{k} \left(\frac{m}{2\pi\hbar^2}\right)^2 \sum_{\lambda v} p_\lambda p_v \sum_{\lambda' v'} |\langle k'v'\lambda'|V|kv\lambda\rangle|^2$$

$$\times\ \delta(\hbar\omega + E_\lambda - E_{\lambda'}) \qquad \text{(I-121)}$$

where k' and k are the final and initial wave vectors of the neutrons, p_λ is the probability that the initial crystal state is λ, p_v is the probability that the initial neutron spin state is v and $\hbar\omega = E$. We take as the effective potential between the neutron and the crystal, the Fermi pseudopotential:

$$V(\underline{r}) = \sum_{\ell} a_{\ell}\delta(\underline{r} - \underline{R}_{\ell}) \quad . \tag{I-122}$$

a_{ℓ} is the scattering length which may change from one atom to another; in particular a_{ℓ} may be different for host and impurity atoms. With these changes, the cross section may be written in the form:

$$\frac{d^2\sigma}{d\Omega dE} = \frac{k'}{k}\left(\frac{m}{2\pi\hbar^2}\right)^2 \frac{1}{2\pi\hbar}\int_{-\infty}^{\infty} dt\, \exp(-i\omega t) \sum_{\lambda} p_{\lambda}$$

$$\times \sum_{\ell\ell'} a_{\ell}^{*}a_{\ell'}\langle\lambda|\exp\{-i\underline{Q}\cdot\underline{R}_{\ell}(0)\}\exp\{i\underline{Q}\cdot\underline{R}_{\ell'}(t)\}|\lambda\rangle$$

where $\underline{Q} = \underline{k}' - \underline{k}$. (I-123)

At this point, the cross section still contains the complete information about the defect configuration and an averaging must be done. What is required is the configuration average of the quantity:

$$\langle a_{\ell}^{*}a_{\ell'}\langle\lambda|\exp\{-i\underline{Q}\cdot\underline{R}_{\ell}(0)\}\exp\{i\underline{Q}\cdot\underline{R}_{\ell'}(t)\}|\lambda\rangle\rangle_{\mathrm{CONF}} \quad . \tag{I-124}$$

However, for simplicity this will be approximated by:

$$\langle a_{\ell}^{*}a_{\ell'}\rangle_{\mathrm{CONF}}\langle\langle\lambda|\exp\{-i\underline{Q}\cdot\underline{R}_{\ell}(0)\}\exp\{i\underline{Q}\cdot\underline{R}_{\ell'}(t)\}|\lambda\rangle\rangle_{\mathrm{CONF}} \quad . \tag{I-125}$$

The second factor is related to the defect crystal Green's function as will be seen below and the averaging is done as in the preceding sections. Assuming a random distribution of defects, the first factor may be written:

$$\begin{aligned} \langle a_\ell^* a_{\ell'} \rangle &= \langle a_\ell^* \rangle \langle a_{\ell'} \rangle \qquad \text{if } \ell \neq \ell' \\ &= \langle |a_\ell|^2 \rangle \qquad \text{if } \ell = \ell' \end{aligned} \tag{I-126}$$

or, assuming that all sites are equal after the averaging:

$$\langle a_\ell^* a_\ell \rangle = \langle a \rangle^2 + \delta_{\ell\ell'} (\langle a^2 \rangle - \langle a \rangle^2) \quad . \tag{I-127}$$

Since we are interested in the coherent scattering, we will retain only that term proportional to $\langle a \rangle^2$ in the cross section.

Finally, for small vibrations, the usual expansion of the exponential terms yields the expression for the coherent inelastic scattering cross section

$$\begin{aligned} \frac{d^2\sigma}{d\Omega dE} = \frac{a^2 k'}{2\pi k} \frac{e^{\beta\omega}}{(e^{\beta\omega}-1)} \sum_{\substack{\alpha\beta \\ \ell\ell'}} Q_\alpha Q_\beta \mathrm{Im} G^A_{\alpha\beta}(\ell\ell';\omega) \\ \times \exp\{i\underline{Q}\cdot(\underline{R}_\ell - \underline{R}_{\ell'})\} \end{aligned} \tag{I-128}$$

where $\hbar\underline{Q}$ and $\hbar\omega$ are the neutron momentum and energy transfer respectively, and a^2 has absorbed the Debye-Waller factor which is assumed constant for all atoms.

It is convenient at this point to write the Green's function in the normal mode coordinates using the transformation (I-39):

$$\mathrm{Im}G_{\alpha\beta}(\ell\ell') = \frac{1}{N}\sum_{\substack{jj'\\ \underline{q}}} \sigma^{*j}_{\alpha}(\underline{q})\,\sigma^{j'}_{\beta}(\underline{q})\,e^{-i\underline{q}\cdot(\underline{R}_{\ell} - \underline{R}_{\ell'})}$$

$$\times\ \mathrm{Im}\tilde{G}^{jj'}(\underline{q},\omega) \qquad \text{(I-129)}$$

where the translational symmetry of the averaged Green's function has been used. Inserting (I-129) into (I-128), we get for the cross section:

$$\frac{d^2\sigma}{d\Omega dE} = \frac{a^2k'}{2\pi k}\,\frac{e^{\beta\omega}}{(e^{\beta\omega}-1)}\sum_{\substack{jj'\\ \underline{q}}} \underline{Q}\cdot\underline{\sigma}^{j*}(\underline{q})\,\underline{Q}\cdot\underline{\sigma}^{j'}(\underline{q})$$

$$\times\ \mathrm{Im}\tilde{G}^{jj'}(\underline{q},\omega)\,\Delta(\underline{k}-\underline{q}) \qquad \text{(I-130)}$$

where $\Delta(\underline{Q}-\underline{q}) = 0$ unless $\underline{k}-\underline{q}$ is a reciprocal lattice vector (the summation on $\underline{q}$ is over the first Brillouin zone, while there is naturally no such restriction on $\underline{Q}$).

Experimentally, the scattering by a given phonon branch j may be examined if the experiment is arranged such that

$$\underline{Q}\cdot\sigma^{j'}(\underline{q}) = 0 \quad \text{for} \quad j' \neq j \quad . \qquad \text{(I-131)}$$

In particular for $\underline{q}$ along a symmetry direction,

$$\frac{d^2\sigma}{d\Omega dE} = \frac{a^2k'}{2\pi k}\,\frac{e^{\beta\omega}}{(e^{\beta\omega}-1)}\,\mathrm{Im}\tilde{G}^{j}(\underline{q},\omega)\,[\underline{Q}\cdot\sigma^{j}(\underline{q})]^2 \quad . \qquad \text{(I-132)}$$

From Eq. (I-102), the imaginary part of the defect crystal Green's function is:

$$\mathrm{Im}\tilde{G}^{j}(\underline{q},\omega) = \frac{\mathrm{Im}\Sigma^{j}(\underline{q},\omega)}{[\omega^2-\omega_j^2(\underline{q})-\mathrm{Re}\Sigma^{j}(\underline{q},\omega)]^2+[\mathrm{Im}\Sigma^{j}(\underline{q},\omega)]^2} \quad . \qquad \text{(I-133)}$$

Thus the peak in the neutron scattering cross section for momentum transfer $\hbar\underline{q}$ can be used to determine the shift in the phonon energies, while the width of the cross section peak can determine the phonon lifetimes. In the case of the perfect crystal, we have:

$$\mathrm{Im}P^{j}(\underline{q},\omega) \propto \delta(\omega^2 - \omega_j^2(\underline{k})) \qquad \text{(I-134)}$$

so that in principle, the neutron should scatter at precisely the energy $\hbar\omega_j(\underline{q})$ given by the perfect crystal phonon dispersion curves, with a peak width equal to zero, i.e., the phonon has infinite lifetime. This is a consequence of the fact that the normal modes of vibration are exact eigenstates of the perfect crystal Hamiltonian. On the other hand, the eigenstates of the defect crystal Hamiltonian are expressed as linear combinations of the single-phonon states whose energies have been renormalized by the real part of the self-energy Σ, while the imaginary part of Σ reflects the spread in the single-phonon states which have been mixed into the eigenstate.

In practice, the perfect crystal cross section peaks will never have zero width, but will have some finite width due to anharmonic effects, random isotopic impurities, etc. Furthermore, a basic width will be introduced due to the resolution limit of the experimental apparatus, involving experimental error in the measurement of neutron wave vectors and energies. When these effects are taken into account, the shifts and widths measured may be compared to the predictions of the low concentration theory presented above.

CHAPTER II

CALCULATIONS

2.1 Single Mass Defect

The details of the calculation of the perfect crystal Green's functions have been described in detail by Bruno (1971). The real and imaginary parts are calculated by:

$$\mathrm{Im}\, P^{R}_{\alpha\beta}(\ell\ell';\omega) = \frac{-\pi}{2\omega}\, \nu_{\alpha\beta}(\ell\ell';\omega) \tag{II-1}$$

and

$$\mathrm{Re}\, P^{R}_{\alpha\beta}(\ell\ell';\omega) = \underline{\underline{P}} \int_{0}^{\omega_{MAX}} \frac{\nu_{\alpha\beta}(\ell\ell';\omega')}{\omega^{2} - \omega'^{2}}\, d\omega' \tag{II-2}$$

where

$$\nu_{\alpha\beta}(\ell\ell';\omega) = \frac{V}{(2\pi)^{3}} \sum_{j} \int d^{3}\underline{k}\; \sigma^{*j}_{\alpha}(\underline{k})\sigma^{j}_{\beta}(\underline{k})\, e^{-i\underline{k}\cdot(\underline{\ell}-\underline{\ell}')}$$

$$\times\ \delta(\omega_{j}(\underline{k}) - \omega) \quad . \tag{II-3}$$

The symbol $\underline{\underline{P}}$ indicates the principle value integral, and the integral over $\underline{k}$ in Eq. (II-3) is performed by the method of Raubenheimer and Gilat (1966) involving a summation over a mesh of points in the irreducible part of the Brillouin zone.

The mean square displacements given by Eq. (I-73) have been calculated for the case of a single gold impurity in a copper host crystal. The parameter ε has the value -2.1, so a resonance is expected in the perfect crystal band. Figures 1 to 4 show the graphs of $\langle u^2(\omega)\rangle$ which are simply proportional to Im G for the particular atom. In Fig. 1 we see $\langle u^2(\omega)\rangle$ at the defect site; also plotted on the same graph (dotted) is $\langle u^2(\omega)\rangle$ for an atom in the pure host crystal. Here the resonance can be clearly seen and in fact, since the resonance frequency is low enough that the perfect crystal density of states is relatively small at this frequency, the result is that the resonance peak is high and narrow indicating that the resonance mode is long-lived with little decay into the band modes. Figures 2 to 4 show $\langle u^2(\omega)\rangle$ for first, second and third nearest neighbours, respectively. In each case, it is the displacement in the plane of the line joining the defect to the neighbour. Figure 2 shows that the effect of the impurity dies off drastically and is already only a minor correction at the first neighbour. The behaviour of $\langle u^2(\omega)\rangle$ at the resonance frequency is easily understood by reference to Eq. (I-77) where the correction term is seen to change sign as ω goes through ω_R thus giving the characteristic wiggle in the spectrum. By the time the third neighbour is reached,

Figure 1

$<u_x^2 \text{ (DEFECT)}>$ (Cu-Au)

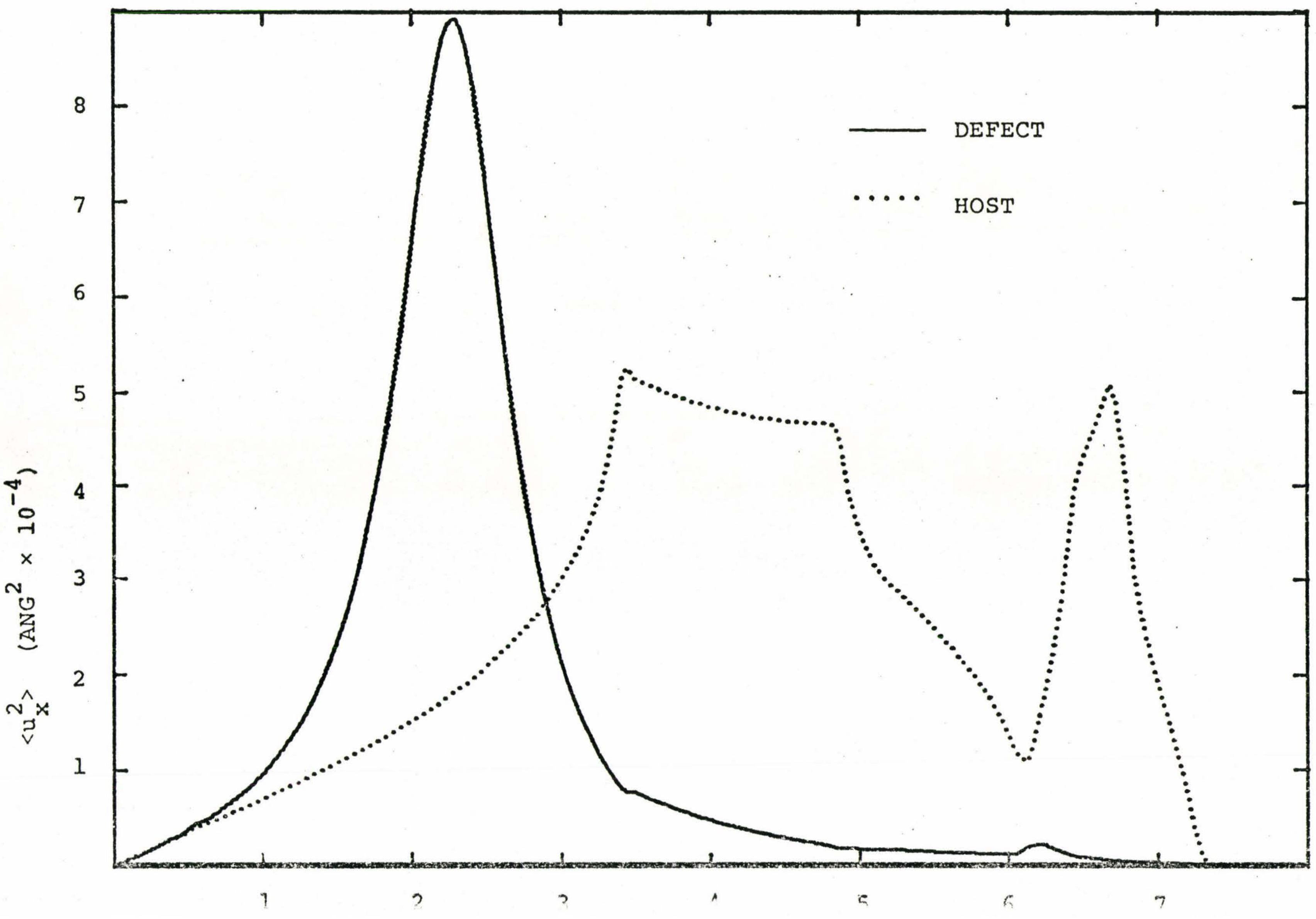

Figure 2

$<u_x^2$ (FIRST NEIGHBOUR)$>$ (Cu-Au)

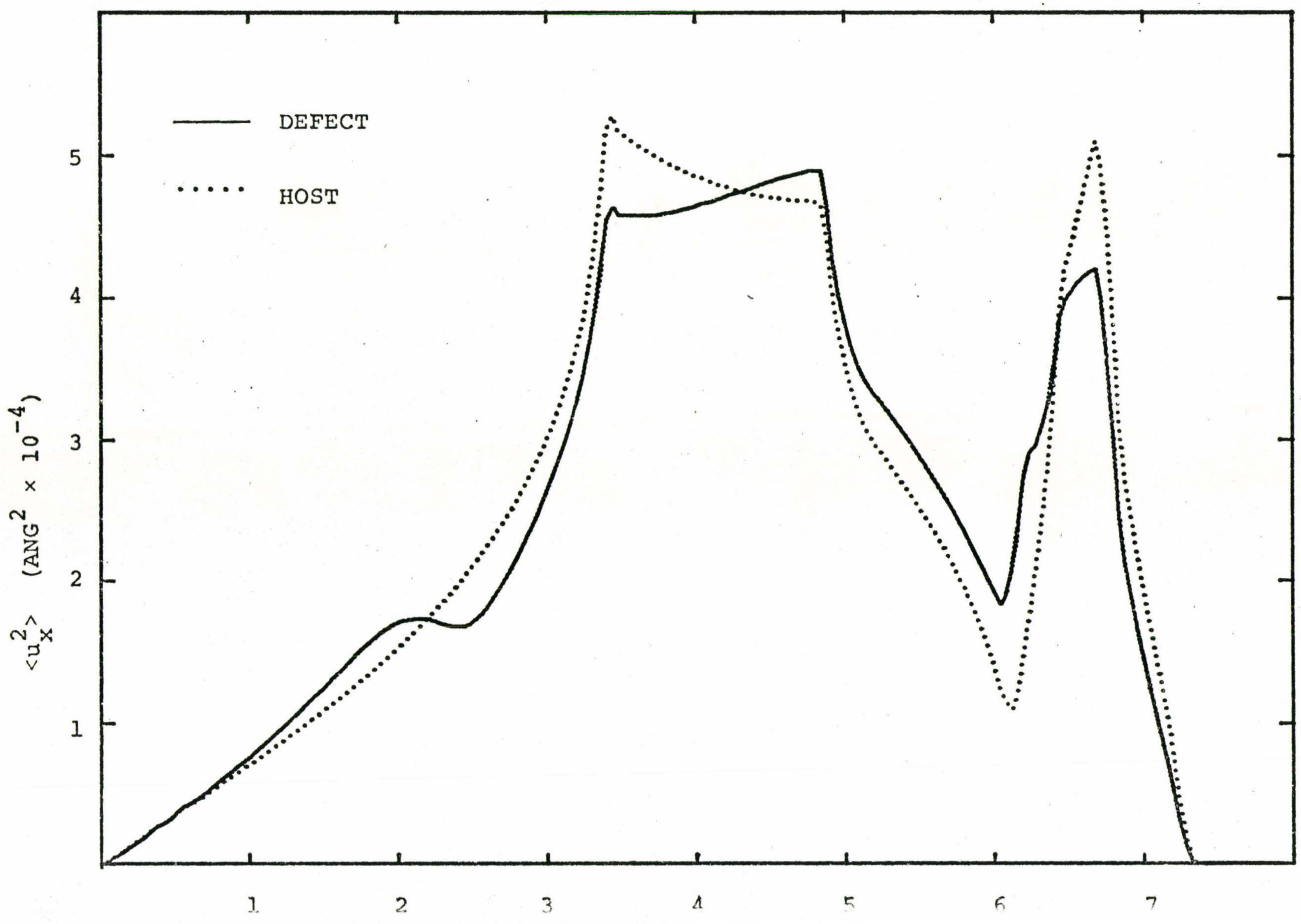

Figure 3

$<u_x^2$ (2ND NEIGHBOUR)$>$ (Cu-Au)

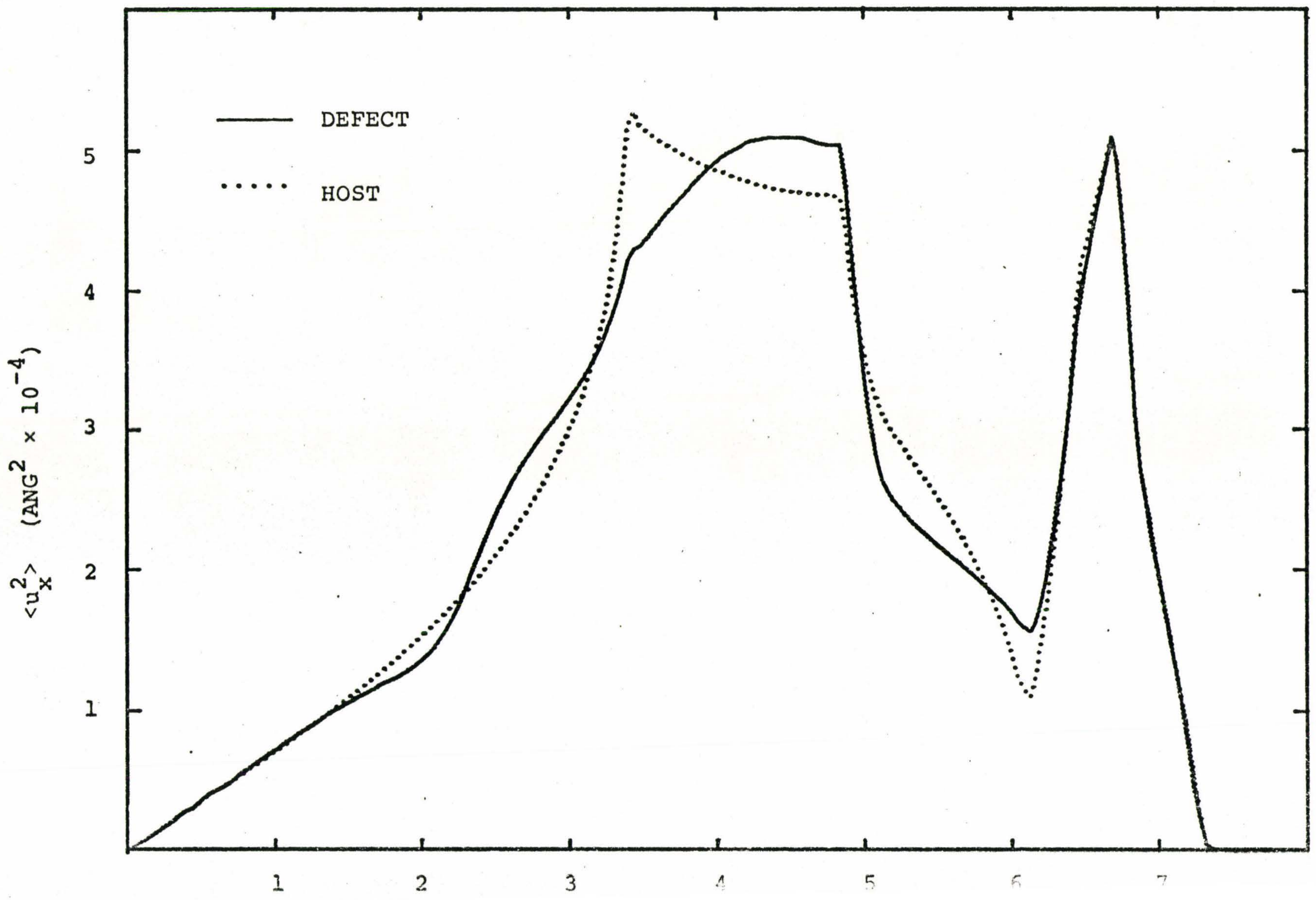

Figure 4

$\langle u_x^2$ (3RD NEIGHBOUR)$\rangle$ (Cu-Au)

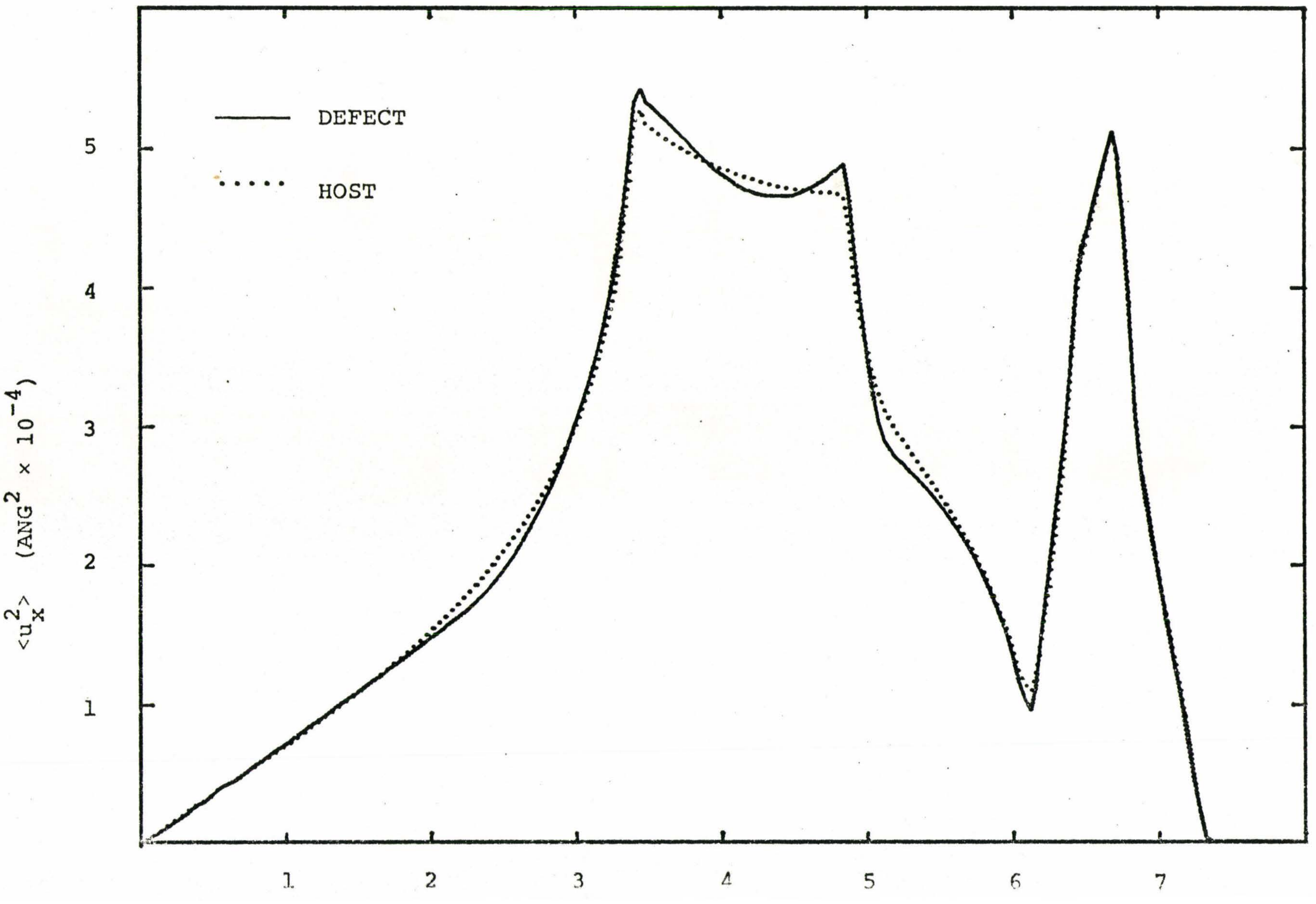

Fig. 4 shows the effect of the impurity to be negligible.

The total displacements $<u^2_{\alpha\alpha}(\ell)>$ are shown in Table 1 for the defect and the first four nearest neighbours. Since the defect is heavier than the host it is natural that the amplitude of vibration of the defect should be smaller than the host. However, what is surprising from this table is that the effect of the impurity is so small even for the nearest neighbours. Of course, if force constant changes were included in the calculation, then the effect would be somewhat greater. Reference to Fig. 2 indicates that even though the spectrum is significantly altered for the first neighbour, the changes are more or less symmetric about the perfect crystal spectrum and so these effects tend to cancel out in the total integral. Thus, if we take this change in the vibration amplitude as some rough measure of the extent of the impurity effects, we may conclude that these effects are of very short range, and this result may support the use of the low concentration theory even at fairly high random concentrations since the assumption is that the defects scatter incoherently.

The same results can be seen for the case of a light defect. Figures 5 to 8 and Table 2 show the calculations for $\varepsilon = .575$ corresponding to an Al defect in Cu. In Table 2, the contribution due to the inband integral has been shown separately from the local mode contribution in order to compare the two contributions.

TABLE 1

MEAN SQUARE DISPLACEMENTS

$\varepsilon = -2.1$	$T = 50°K$
	($ANG^2 \times 10^{-3}$)
$<u_x^2$ (DEFECT)$>$	1.5287
$<u_x^2$ (1)$>$	2.1317
$<u_z^2$ (1)$>$	2.1330
$<u_z^2$ (2)$>$	2.1335
$<u_x^2$ (2)$>$	2.1320
$<u_x^2$ (3)$>$	2.1343
$<u_y^2$ (3)$>$	2.1353
$<u_z^2$ (3)$>$	2.1353
$<u_x^2$ (4)$>$	2.1329
$<u_z^2$ (4)$>$	2.1321
$<u_\alpha^2$ (HOST)$>$	2.1383

Figure 5

$\langle u_x^2$ (DEFECT)$\rangle$ (Cu-Aℓ)

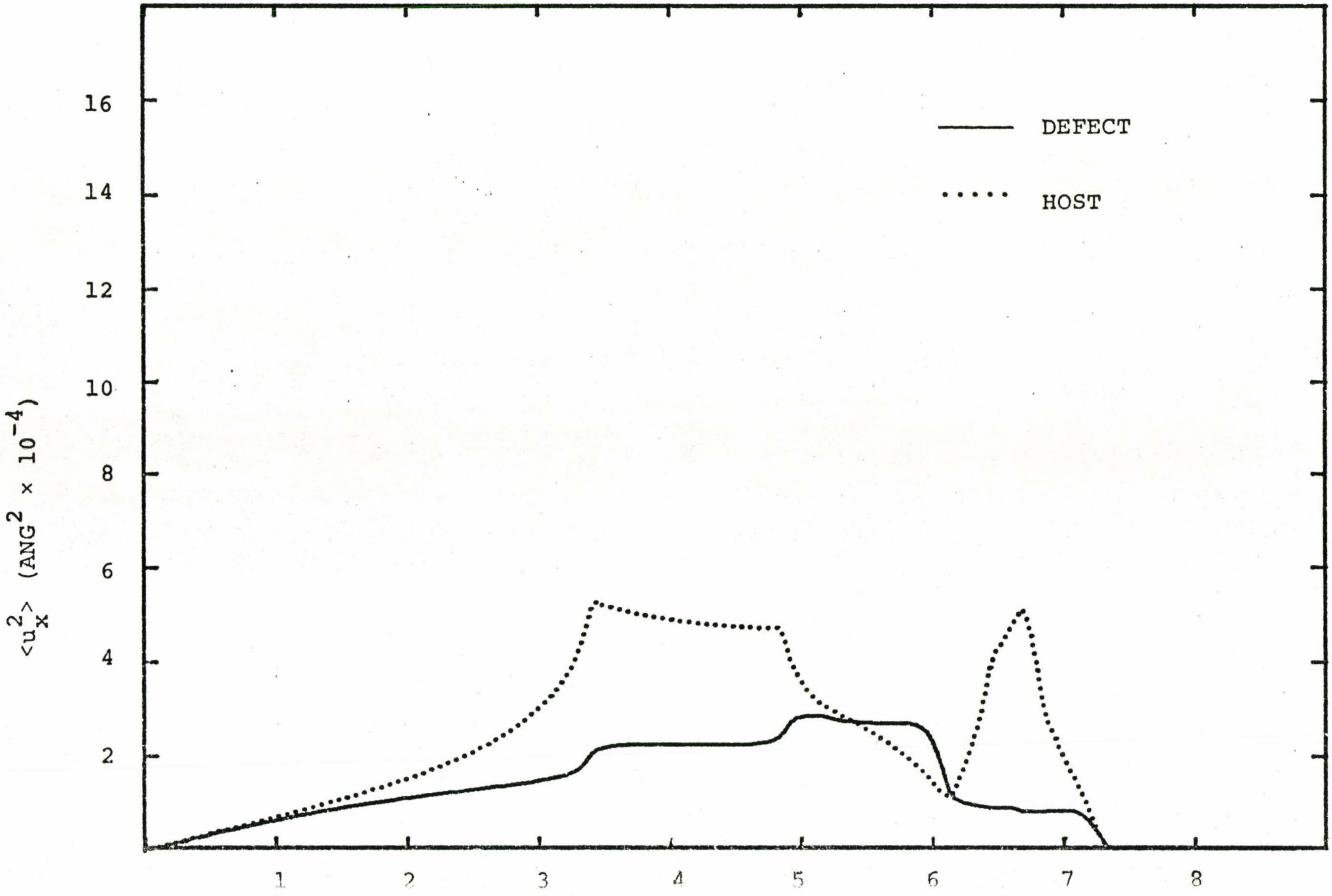

Figure 6

$\langle u_x^2$ (FIRST NEIGHBOUR)$\rangle$ (Cu-Aℓ)

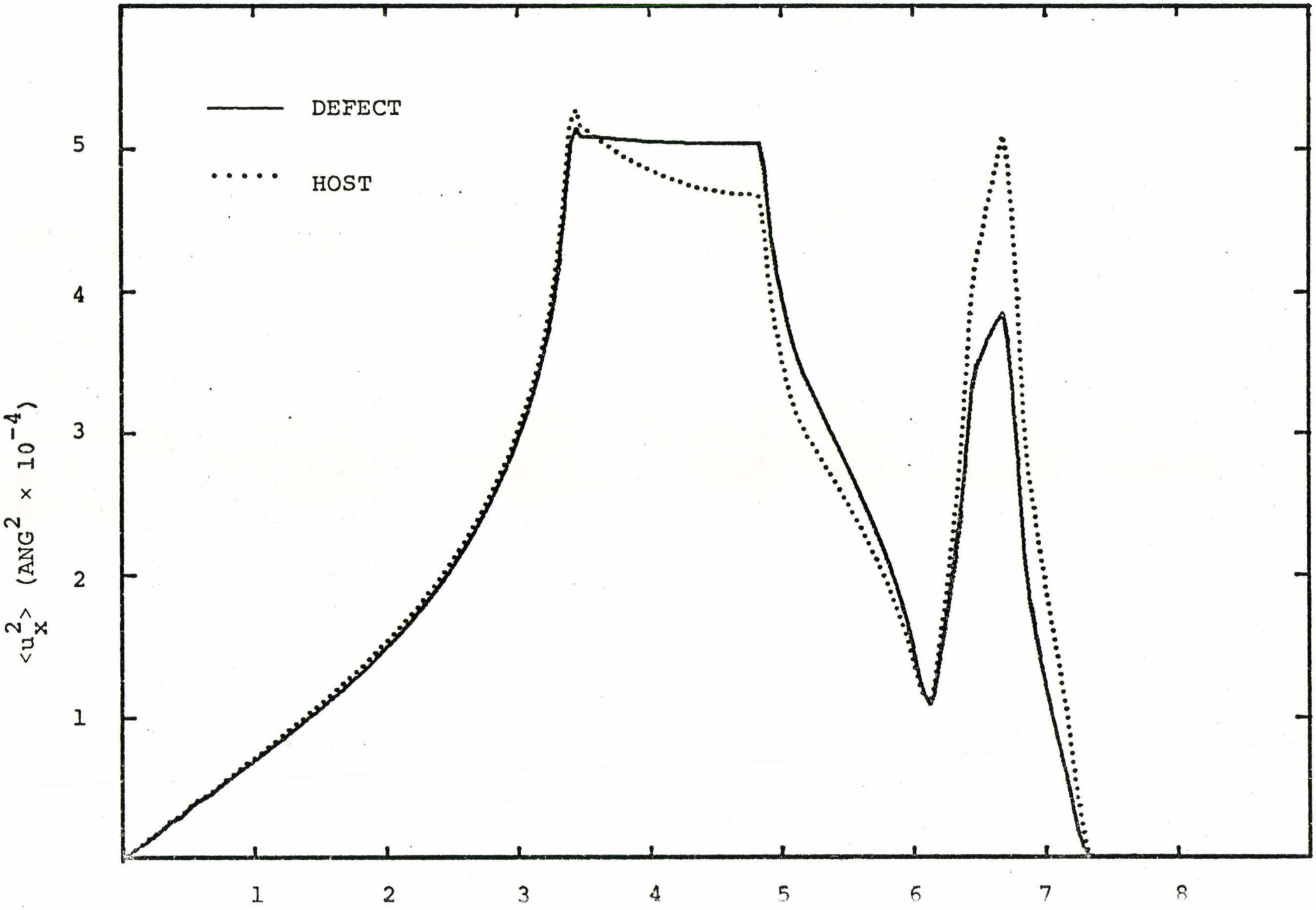

Figure 7

$<u_x^2$ (2ND NEIGHBOUR)$>$ (Cu-Aℓ)

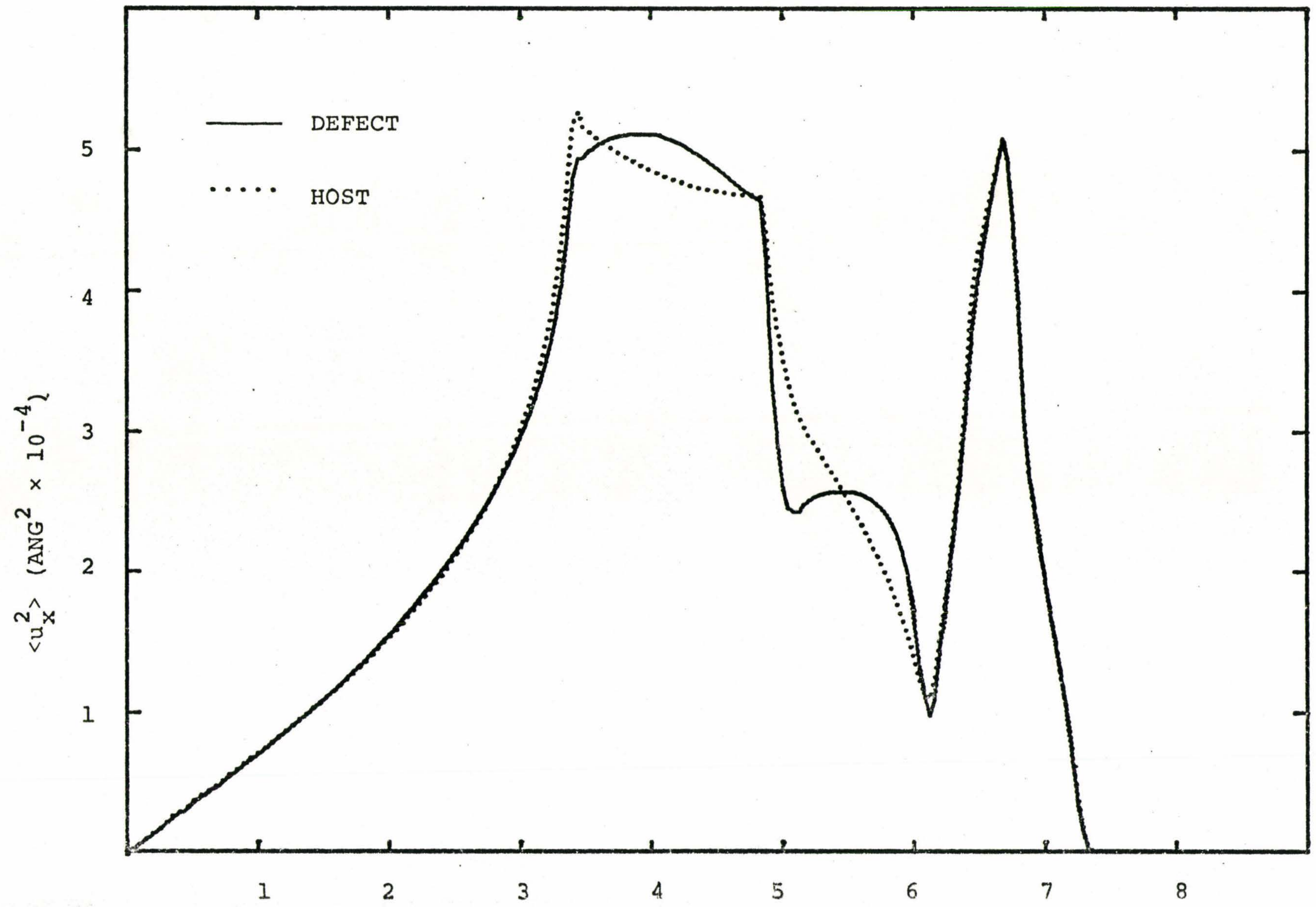

Figure 8

$<u_x^2$ (3RD NEIGHBOUR)$>$ (Cu-Aℓ)

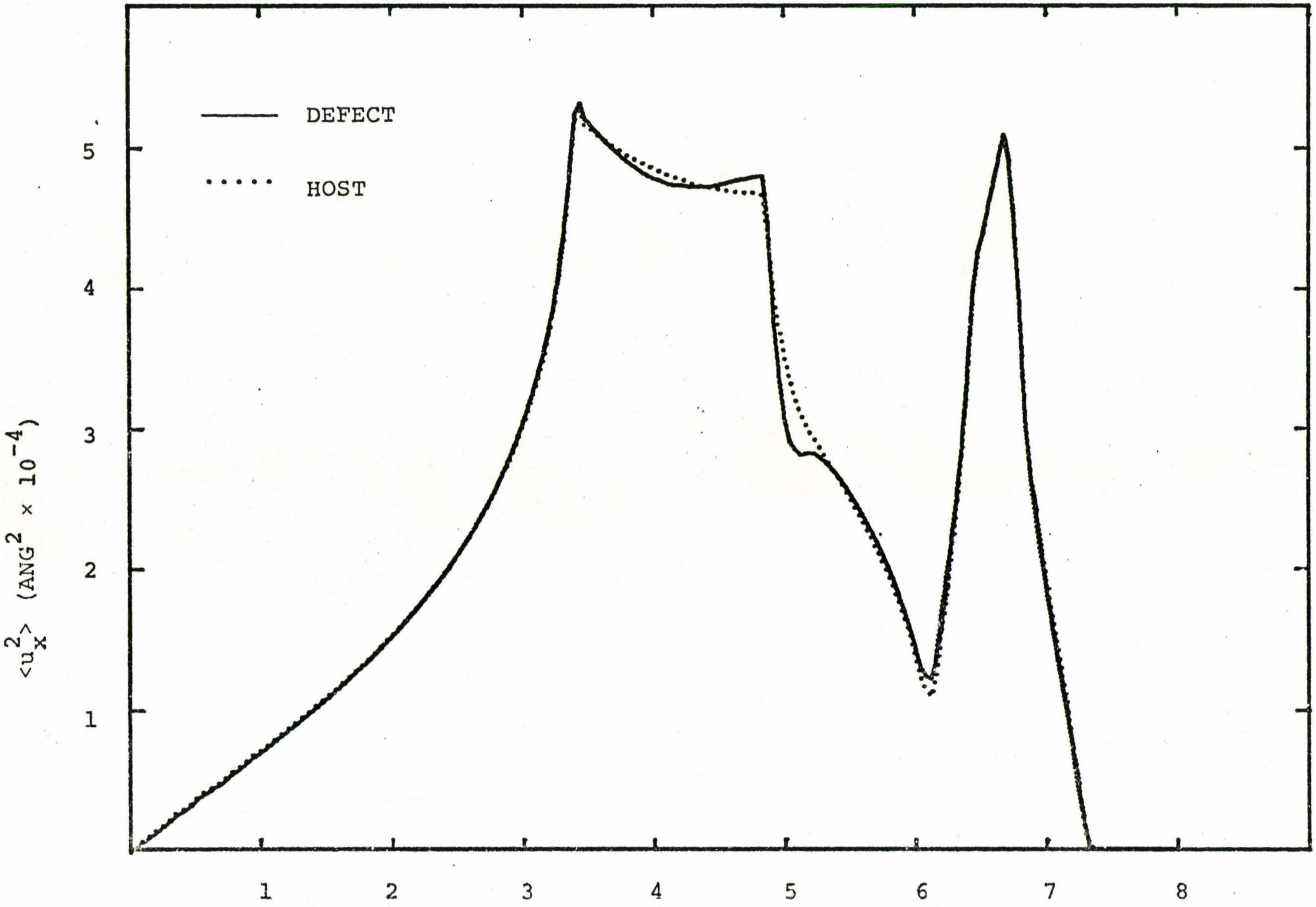

TABLE 2

MEAN SQUARE DISPLACEMENTS

$\varepsilon = .575$ T = 50°K

	INBAND CONTRIBUTION $(\text{ANG}^2) \times 10^{-3}$	LOCAL MODE CONTRIBUTION $(\text{ANG}^2) \times 10^{-3}$	TOTAL $(\text{ANG}^2) \times 10^{-3}$
$\langle u_x^2$ (DEFECT)$\rangle$	1.3018	1.60116	2.9029
$\langle u_x^2$ (1)$\rangle$	2.1118	.00267	2.1385
$\langle u_z^2$ (1)$\rangle$	2.1335	.00017	2.1352
$\langle u_z^2$ (2)$\rangle$	2.1367	1.2×10^{-5}	2.1367
$\langle u_x^2$ (2)$\rangle$	2.1333	2.98×10^{-4}	2.1336
$\langle u_x^2$ (3)$\rangle$	2.1361	1.86×10^{-4}	2.1363
$\langle u_y^2$ (3)$\rangle$	2.1363	2.45×10^{-4}	2.1365
$\langle u_z^2$ (3)$\rangle$	2.1363	2.45×10^{-4}	2.1365
$\langle u_x^2$ (4)$\rangle$	2.1342	6.90×10^{-4}	2.1348
$\langle u_z^2$ (4)$\rangle$	2.1330	7.67×10^{-5}	2.1331
$\langle u_x^2$ (HOST)$\rangle$	2.1383	0	2.1383

The local mode contribution has been calculated by evaluating the imaginary part of the Green's function at $\omega = \omega_L$. Since ω_L is above the perfect crystal density of states maximum, it follows that $\mathrm{Im}\,P(\omega_L) = 0$, and Im G can be found from Eq. (I-70) by adding a small imaginary part to : $\omega \rightarrow \omega + i\delta$, where $\delta \rightarrow 0^+$. Then Im G can be shown to be:

$$\mathrm{Im}\,G_{\alpha\beta}(\ell\ell';\omega) = \frac{-\pi\varepsilon\omega_L^2\,\delta(\omega-\omega_L)}{[\frac{-2}{\omega_L} + 2\varepsilon\omega_L^3 \int \frac{\nu(\omega')d\omega'}{(\omega_L^2 - \omega'^2)^2}]}$$

$$\times \sum_\gamma \mathrm{Re}\,P_{\alpha\gamma}(\ell 0;\omega_L)\,\mathrm{Re}\,P_{\gamma\beta}(0\ell';\omega_L) \qquad \text{(II-4)}$$

and the contribution to the local mode is, from (I-73):

$$\langle u_\alpha(\ell)u_\beta(\ell')\rangle = \frac{h\varepsilon\omega_L^2 \coth(\beta\omega_L/2)}{[\frac{-2}{\omega_L} + 2\varepsilon\omega_L^3 \int \frac{\nu(\omega')d\omega'}{(\omega_L^2 - \omega'^2)^2}]}$$

$$\times \sum_\gamma \mathrm{Re}\,P_{\alpha\gamma}(\ell 0;\omega_L)\,\mathrm{Re}\,P_{\gamma\beta}(0\ell';\omega_L) \quad . \qquad \text{(II-5)}$$

Once again, the spectrum is drastically altered at the defect site. In fact, Fig. 5 and Table 2 show that the contribution from the single local mode frequency outweighs the whole inband contribution. However, as we go down through the neighbours, the local mode contribution becomes negligible (.1% at the first neighbour) and the spectrum looks like that for $\varepsilon = -2.1$, except that the resonance effect is missing for the light impurity.

Thus, for both the light and heavy mass defect, the effect of the impurity dies away so quickly that it is felt significantly by only the first neighbour. In fact even for the first neighbour, when the total displacement is changed by 30% at the defect site, the change in that neighbour's displacement is about .3%. The changes in the spectrum can be seen at the first neighbour, especially in the region of the resonance, but then changes will tend to cancel in calculating any physical property involving the integral over frequency.

To extend this argument to the case of a point defect with small nearest neighbour force constant changes, it would seem reasonable to assume that the effects of the impurity would be felt significantly at the defect and neighbour with slight perturbation at the second neighbour. However, this calculation has not been done here, so all that can be argued is that physically, one would expect the force constant changes to shift the resonance, and to extend the effect of the impurity due to the larger defect space, but not to extend these effects much beyond the defect space, since the mass defect is incapable of doing this, as has been shown. The significance of this result is to lend support to the use of the low concentration theory, which will break down when the coherent scattering of phonons off clusters becomes significant. We conclude that these clusters must be extremely close together to cause coherent scattering, which means that the concentration must be fairly high.

2.2 Copper-Gold Alloy

The low concentration theory has been used to calculate the shifts and widths of the phonons in an alloy consisting of 3% gold in copper. This system has $\varepsilon = -2.1$ so no local mode exists, and the low concentration makes it suitable for this theory. Furthermore, the shifts and widths have been measured experimentally by Svensson and Kamitakahara (1971) for $\underline{q}$ in the directions T(z00) and T1(zz0) [eigenvector $(1/\sqrt{2}, -1/\sqrt{2}, 0)$], and in the T(zzz) direction, though this result is not published as yet. Calculations have been done on this system by Bruno and Taylor (1971) and most recently, Kesharwani and Agrawal (1973) for the T(z00) and T1(zz0) branches. No calculations in the T(zzz) direction have yet been reported.

The self energy is calculated using the perturbation theory, Eq. (I-120), as described in Appendix I, where it is assumed that only nearest neighbour force constant changes are involved. The pure copper force constants fitted by Svensson and Kamitakahara (1971) were used, as modified by Bruno and Taylor (1971) to account for the overall expansion of the lattice, which is about 1.6% at c = 3%. The imaginary part of $\tilde{G}^j(\underline{q},\omega)$ was then calculated using (I-133).

It has been shown, (I-130), that the neutron scattering cross section is proportional to Im $\tilde{G}^j(\underline{q},\omega)$. In fact, it is the peak in Im $\tilde{G}^j$ which determines the peak in the scattering cross section. It can be seen from (I-133) that Im $\tilde{G}$ would be Lorentzian in ω if $\Sigma^j(\underline{q},\omega)$ were independent of ω. In the lowest approximation, we set $\omega = \omega_j(\underline{q})$ in Σ, and there the peak can be shown to occur at

$$\omega \approx \omega_j(\underline{q}) + \frac{\text{Re } \Sigma^j(\underline{q},\omega_j(\underline{q}))}{2\omega_j(\underline{q})} \tag{II-6}$$

while the half-width at half-maximum is given approximately by:

$$\Gamma \approx \frac{\text{Im } \Sigma^j(\underline{q},\omega_j(\underline{q}))}{2\omega_j(\underline{q})} \quad . \tag{II-7}$$

However, since Σ is not independent of ω, the peak tends to be more assymetric and it becomes necessary to define the peak to be the center of the half-maximum points of the full function (I-133) in order to conform with the experimental method of Svensson and Kamitakahara. This procedure involves calculating the function $\tilde{G}(\underline{q},\omega)$ at many values of ω for each $\underline{q}$ and performing some kind of operational measurement of the peak position and size, so it is obviously more time consuming. The approximation (II-6) involves the value of Σ on the energy shell and will be referred to below as the "on-shell calculation", while the operational procedure will be referred to as the "off-shell calculation".

The two procedures are compared in Figs. 9 and 10 which show the on-shell and off-shell calculations of the

Figure 9

FREQUENCY SHIFTS ON T1(zz0) BRANCH

ONSHELL AND OFFSHELL

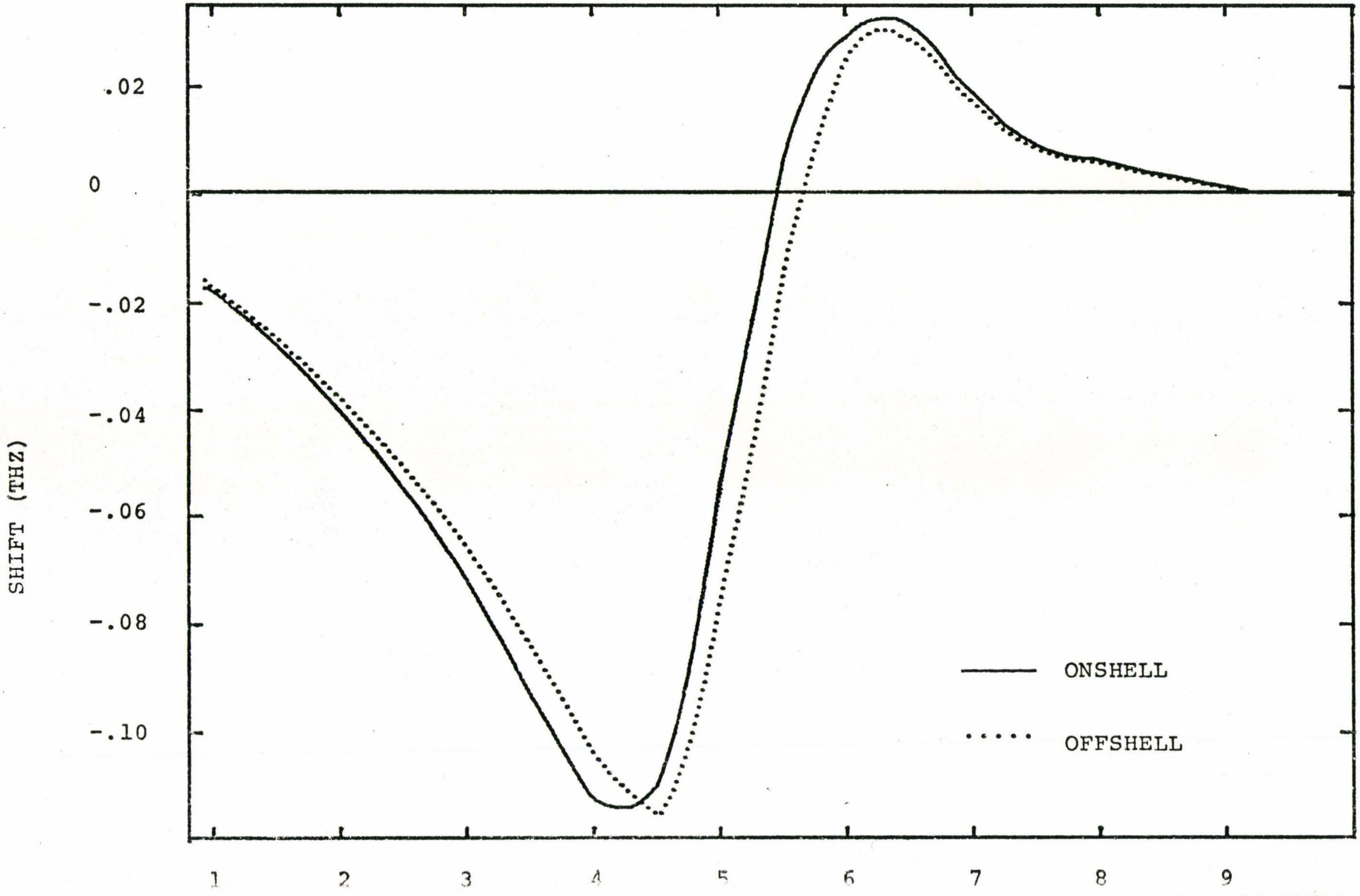

Figure 10

FREQUENCY SHIFTS ON T(zzz) BRANCH

ONSHELL AND OFFSHELL

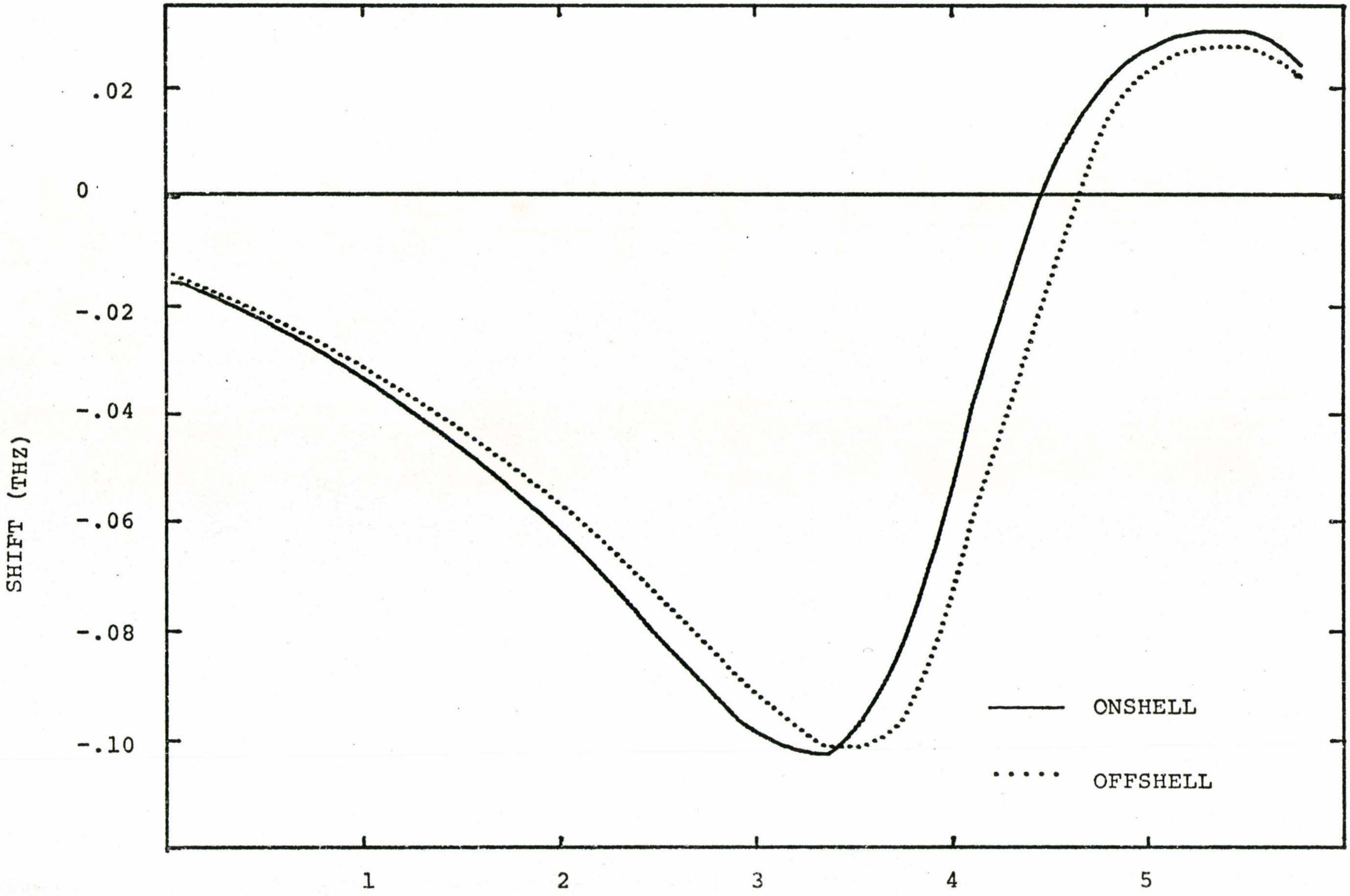

frequency shifts in the Tl(zz0) and T(zzz) branches respectively. The force constant changes used are those of Bruno (1971) (see below). The off-shell results were calculated by evaluating Im $\tilde{G}(\underline{k})$ at 100 points within a window of about 5Γ centred on the peak, where the peaks and Γ were calculated with the on-shell method. Im G was then interpolated linearly and the shifts and widths were measured. We can see from the figures that in both directions, the two methods differ somewhat especially in the regions where the shifts are largest in magnitude. However, as $\omega \to 0$, the two methods converge. These differences reflect the asymmetry of the peaks due to the ω-dependence of Σ, and are sufficient to warrant the use of the off-shell method for comparison with experiment at high ω, while the on-shell method should be satisfactory for $\omega \to 0$.

2.3 Elastic Constants

The frequency shifts for k → 0 can be used to calculate the elastic constants of the alloy, as has been done by Kesharwani and Agrawal (1972) for dilute Mo-Re alloys. In the symmetry directions, the elastic constants are related to the velocity of sound by

$$c_s = \rho v_s^2 \qquad \text{(Kittel (1968))} \qquad \text{(II-8)}$$

where ρ is the density and v_s is the velocity of the acoustic wave in the mode appropriate for the elastic constant required. In particular, for cubic crystals:

$$c_{44} = \rho v^2_{T(z00)} = \rho v^2_{T2(zz0)} \qquad \text{(II-9)}$$

$$c_{11} = \rho v^2_{L(z00)} \qquad \text{(II-10)}$$

$$c' = \frac{1}{2}(c_{11} - c_{12}) = \rho v^2_{T1(zz0)} \quad . \qquad \text{(II-11)}$$

The sound velocities can be determined from the dispersion curves of the crystal:

$$v_s = \frac{\partial \omega_s(\underline{k})}{\partial \underline{k}} \quad , \quad \underline{k} \to 0 \qquad \text{(II-12)}$$

$$\simeq \frac{\omega_s(\underline{k})}{k} \qquad \text{for long wavelengths} \quad . \qquad \text{(II-13)}$$

In the dilute alloy, for small changes in the parameters involved, we can write:

$$\frac{\Delta v_s}{v_s} = \frac{\Delta\omega_s(\underline{k})}{\omega_s(\underline{k})} - \frac{\Delta k}{k} \quad . \qquad \text{(II-14)}$$

But the change in wave vector is related to the change in the lattice parameter by:

$$k = \frac{2\pi z}{a}$$

which gives:

$$\frac{\Delta k}{k} = - \frac{\Delta a}{a} \quad . \qquad \text{(II-15)}$$

so that from Eq. (II-14), we get finally:

$$\frac{\Delta c_s}{c_s} = \frac{\Delta\rho}{\rho} + 2 \left[\frac{\Delta\omega_s(z)}{\omega_s(z)} + \frac{\Delta a}{a}\right] \quad . \qquad \text{(II-16)}$$

As $z \to 0$, $\Delta\omega_s(z)/\omega_s(z)$ becomes independent of z. To see how low it is necessary to go in order to get linearity in the shifts, Table 3 shows $\Delta\omega/\omega$ calculated using the force constant changes of Bruno and Taylor (1971). We can see from the table that $\Delta\omega/\omega$ is linear to about .003% by the time ω is down to about 10^{-3} THz. This accuracy is limited by the numerical methods used in computing the shifts. However, in view of the approximations inherent in the perturbation

TABLE 3

$\Delta\omega/\omega$ FOR $z \to 0$

ω	$\Delta\omega/\omega$ - T1(110)	ω	$\Delta\omega/\omega$ - T(zzz)
.629	-.037762	1.02	-.03428096
$.613 \times 10^{-1}$	-.03628096	.103	-.02937061
$.613 \times 10^{-2}$	-.03627197	$.103 \times 10^{-1}$	-.02932597
$.613 \times 10^{-3}$	-.03627201	$.103 \times 10^{-2}$	-.02932590
$.613 \times 10^{-4}$	-.03627201	$.103 \times 10^{-3}$	-.02932607

approach, especially at low ω, this accuracy is obviously sufficient.

The elastic constants of Cu-(2.8 at.%)Au have been measured by O'Hara and Marshall (1971) at various temperatures and can be used to compare with the predictions of the low concentration theory. The results reported by O'Hara and Marshall are shown in Table 4 where the elastic constants for pure copper are those reported by Overton and Gaffney (1955), since O'Hara and Marshall have not reported these. The other relevant parameters for Eq. (II-16) have been given by O'Hara and Marshall as:

$$\Delta a/a = 4.7 \times 10^{-3} \quad \text{at} \quad c = .028$$

and

$$\Delta \rho/\rho = .044 \quad .$$

Before using $\Delta\omega/\omega$ from Table 3, it is important to account for the finite frequency shift due to the overall expansion of the lattice, as evidenced by the change in the lattice parameter a. In fact, the shifts in Table 3 are measured with respect to the frequencies calculated at the new lattice parameter and not with respect to those of pure copper. The additional shift due to the lattice expansion

TABLE 4

ELASTIC CONSTANTS MEASURED BY O'HARA AND MARSHALL AT T = 300°K IN UNITS OF 10^{11} DYN/CM^2

% Au	c_{11}	c_{44}	$c' = \frac{1}{2}(c_{11}-c_{12})$	c_{12}
0 %	16.839	7.539	2.348	12.142 [a]
0.23%	17.000	7.419	2.340	12.320
2.8 %	16.917	7.392	2.265	12.387
10.0 %	17.467	7.313	2.186	13.095

[a] 0% Au measurements by Overton and Gaffney (1955).

can be expressed in terms of the mode Gruneisen parameter γ by:

$$\Delta\omega_j(z) = \omega_j(z)\gamma_j(z) \frac{\Delta V}{V} \tag{II-17}$$

where

$$\gamma_j(z) = \frac{\partial \ \ell n \ \omega_j(z)}{\partial \ \ell n \ V} \ . \tag{II-18}$$

These have been measured in the limit z → 0 by Daniels (1965) for copper and have the values:

$$\gamma_{T1}(zz0) = 1.49$$

$$\gamma_L(z00) = 2.48$$

and $\gamma_{T2}(zz0) = 1.92$

for the modes which will be of interest here.

It was decided to assume that the force constant changes were central, satisfying:

$$\Delta 1XX - \Delta 1XY = \Delta 1ZZ \tag{II-19}$$

where $\Delta 1XX$ is the change in the force constant between the defect and the nearest neighbour at $\underline{\ell} = a/2\ (1, 1, 0)$. These are related to what Agrawal (1973) calls the central and non-central force constants A and B respectively by:

$$\Delta A = \Delta 1XX + \Delta 1XY \qquad \text{(II-20)}$$

$$\Delta B = \Delta 1ZZ \quad . \qquad \text{(II-21)}$$

There are two reasons why central forces were assumed. First, the c_{11} elastic constant can only be calculated by knowing the frequency shifts along the longitudinal branches, and it is precisely along these branches that it might be expected that second and third neighbour force constant changes play a significant role, making this simple calculation unreliable. Secondly, the experimental results of O'Hara and Marshall show that c_{11} is not a monotonic function of concentration, which, if not casting suspicion on the results, at least rules out the possibility of explaining it with a theory linear in the concentration. So this leaves two elastic constants which can fit unambiguously the two central force constant changes.

The elastic constant changes Δc_{44} and $\Delta c'$ were calculated by Eq. (II-16) in the T1(zz0) and T2(zz0) branches for various sets of central force constant changes. Table 5 shows some of the results used in the fitting. We can see from the table that the elastic constant changes vary

TABLE 5

CALCULATION OF ELASTIC CONSTANT CHANGES

CENTRAL CONDITION: $\Delta 1ZZ = \Delta 1XX - \Delta 1XY$

$\Delta 1XX$ $(THz)^{-2}$	$\Delta 1ZZ$ $(THz)^{-2}$	$\Delta c_{44}/c_{44}$	$\Delta c'/c'$
50	-5.23	-.0412	-.0217
75	-5.23	-.0311	-.00306
100	-5.23	-.0210	.0156
125	-5.23	-.0109	.0342
50	-5	-.0411	-.0212
50	0	-.0391	-.0100
50	5	-.0371	.00118
50	10	-.0351	.01235

almost linearly with the force constant changes, which makes the fitting procedure straightforward. Table 6 shows the final fitted force constant changes along with the elastic constant changes calculated from them. The other force constant changes included are those fitted by Bruno and Taylor (1971), and those of Kesharwani and Agrawal (1973).

The fitted force constant changes are very large compared with the other two sets. In particular Δ1ZZ is a change of 480% from the pure copper, while Δ1XX and Δ1XY are 120% and 138% respectively. These results seem very unphysical, in view of the changes calculated by various authors using phenomenological models (e.g., Kesharwani and Agrawal (1973)). Furthermore, the validity of the perturbation approach becomes doubtful with such large changes. It may be that the second and further neighbour changes are significant at these long wavelengths and that these large values result from trying to force the nearest neighbour changes to account for all the elastic constant change. Also, it may be useful to relax the central forces condition, especially since the measured force constants of the pure copper are non-central.

At any rate, it is obvious that neither the force constant changes of Bruno and Taylor nor those of Kesharwani and Agrawal come close to calculating the correct elastic constant changes, although Kesharwani is somewhat better Bruno. In fact, although the c_{11} elastic constant was not

TABLE 6

COMPARISON OF EXPERIMENTAL AND CALCULATED ELASTIC CONSTANT CHANGES

	Δ1XX (THz)$^{-2}$	Δ1ZZ (THz)$^{-2}$	Δ1XY (THz)$^{-2}$	$\Delta c_{44}/c_{44}$	$\Delta c'/c'$	$\Delta c_{11}/c_{11}$
	-	EXPERIMENTAL	-	-.0199	-.034	.004
FITTED:	137.3	-39.8	177.1	-.0199	-.034	-.0196
BRUNO:	22.28	5.21	41.99	-.0515	-.061	-.0695
AGRAWAL:	58.75	- 2.5	61.25	-.0394	-.012	-.0540

used in the fitting, it turns out that the fitted changes give a much better result in this direction than either of the other two. At any rate, the final evaluation of the fitted changes must be the comparison with the shifts and widths measured throughout the entire frequency range.

2.4 Calculation of Shifts and Widths

The shifts and widths have been calculated for the three sets of force constant changes, and are shown in Figs. 11 to 13 for the shifts in the T(z00), T(zzz) and Tl(zz0) branches respectively, and in Figs. 14 to 16 for the half-widths at half-maximum in the T(z00), T(zzz) and Tl(zz0) branches. In these calculations the effect of the volume change due to the impurities has not been included.

Figures 11 to 13 show that the shifts are considerably affected by changing the force constant changes. For the T(z00) and T(zzz) directions, the shifts due to Kesharwani's changes tend to follow quite closely those of the fitted changes, while in the Tl(zz0) direction, both shifts differ from those of Bruno as well as each other. It can be seen that the stiffening of the force constants in the case of Kesharwani and the fitted changes has resulted in a general decrease in the low frequency shifts and has moved the resonance to slightly higher frequencies (see widths), while enhancing the resonance in general. The effect on the low frequency end in the T(z00) and Tl(zz0) directions can be understood since it was necessary to decrease the shift as ω tended to zero in order to fit the elastic constant data (cf. Table 5).

Since the shifts due to Bruno's changes have been shown to fit the experimental data in the T(z00) and Tl(zz0)

FIGURE 11

FREQUENCY SHIFTS IN T(z00) DIRECTION (NO VOLUME EFFECT)

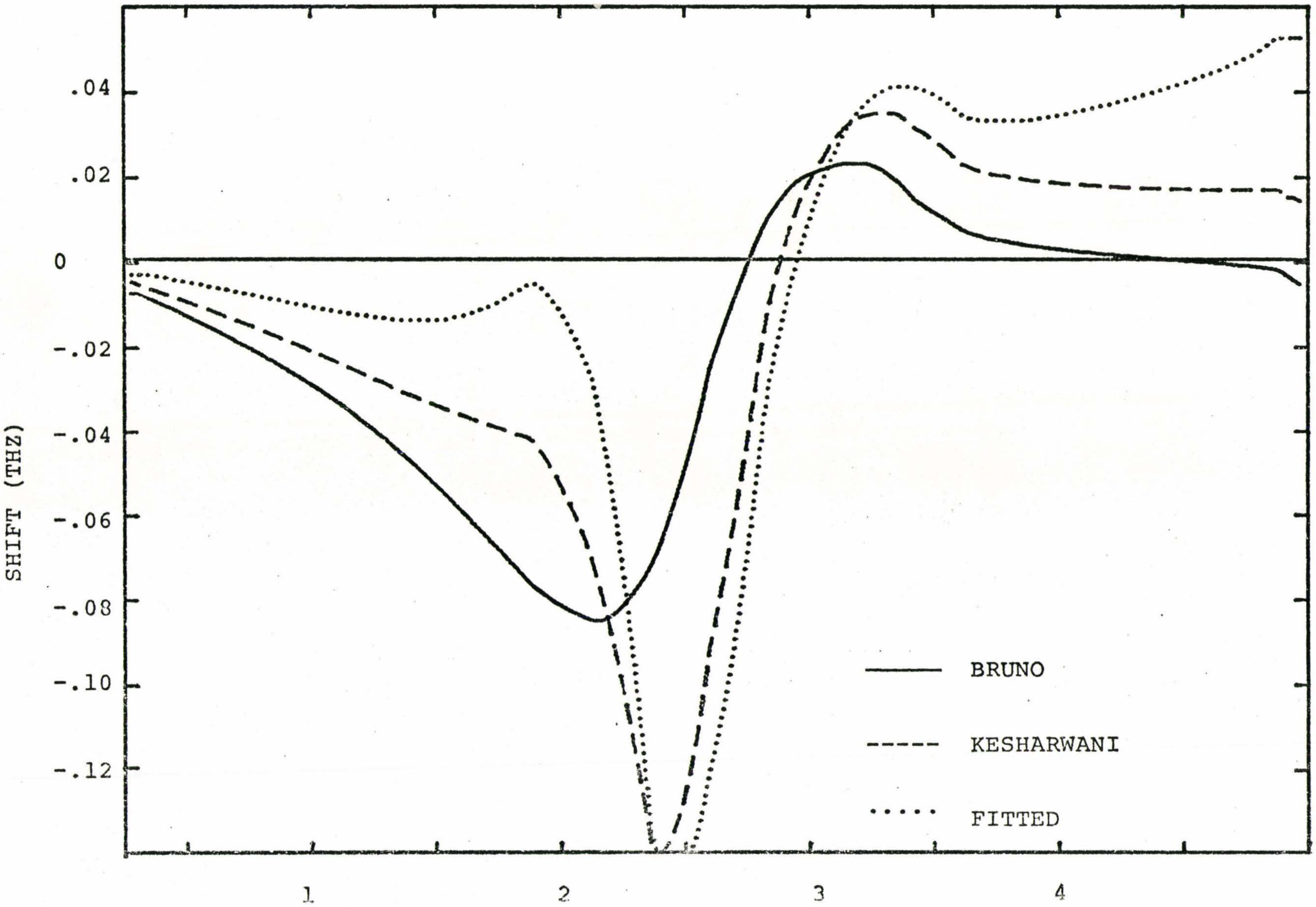

FIGURE 12

FREQUENCY SHIFTS IN T(zzz) DIRECTION (NO VOLUME EFFECT)

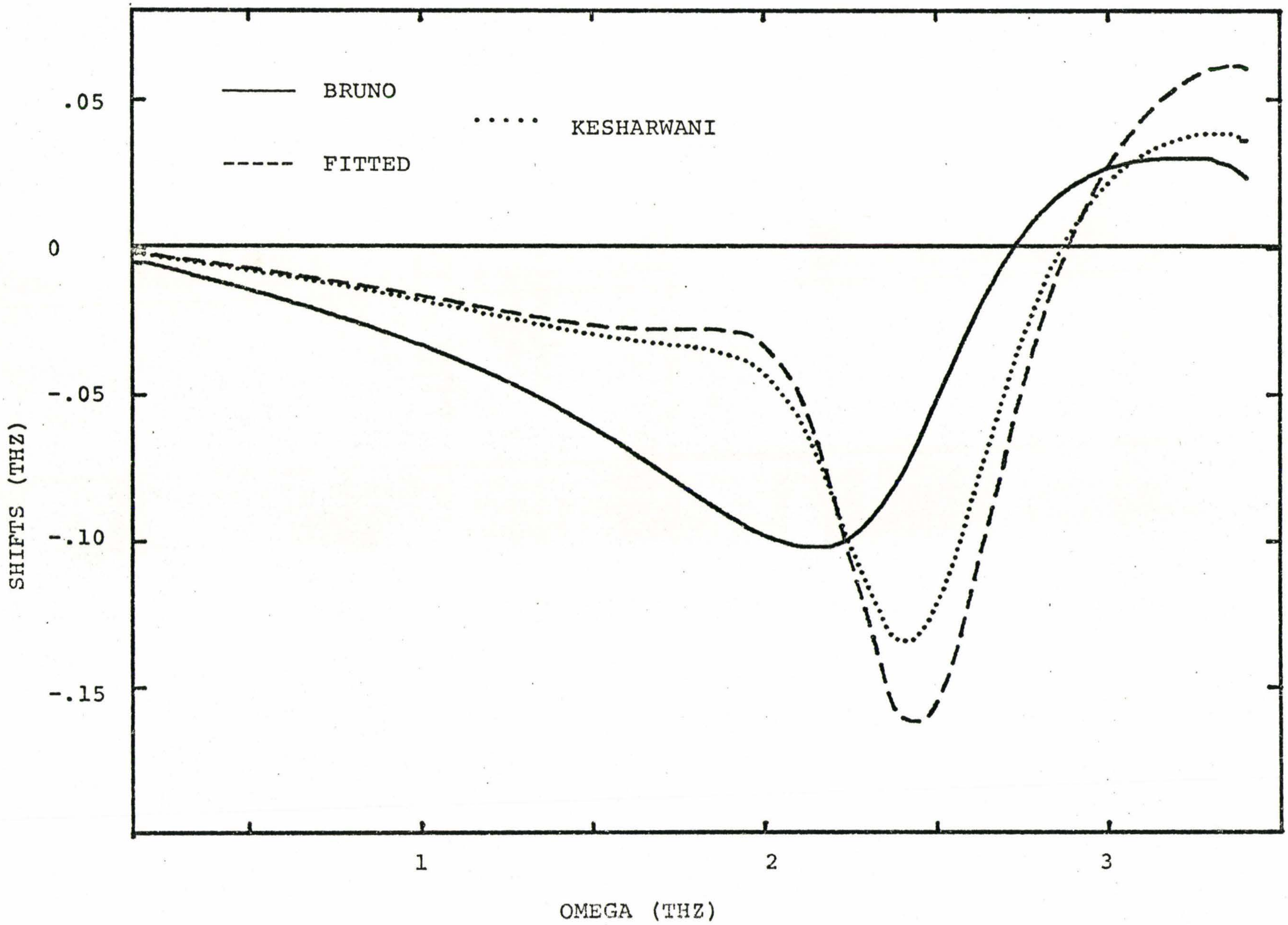

FIGURE 13

FREQUENCY SHIFTS IN T1(zz0) DIRECTION (NO VOLUME EFFECT)

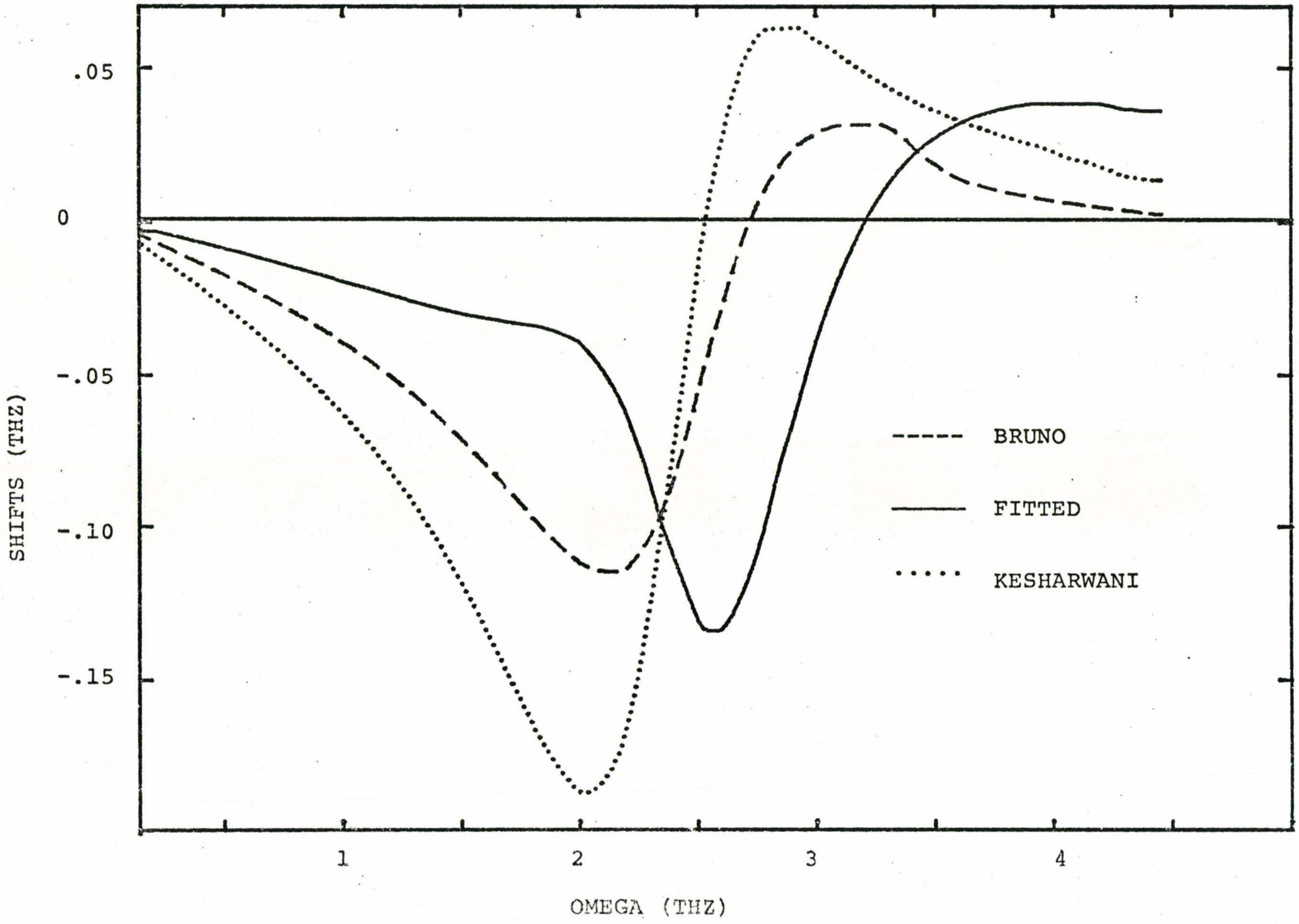

FIGURE 14

HALF-WIDTHS AT HALF-MAXIMUM IN T(z00) DIRECTION (NO RESOLUTION EFFECT)

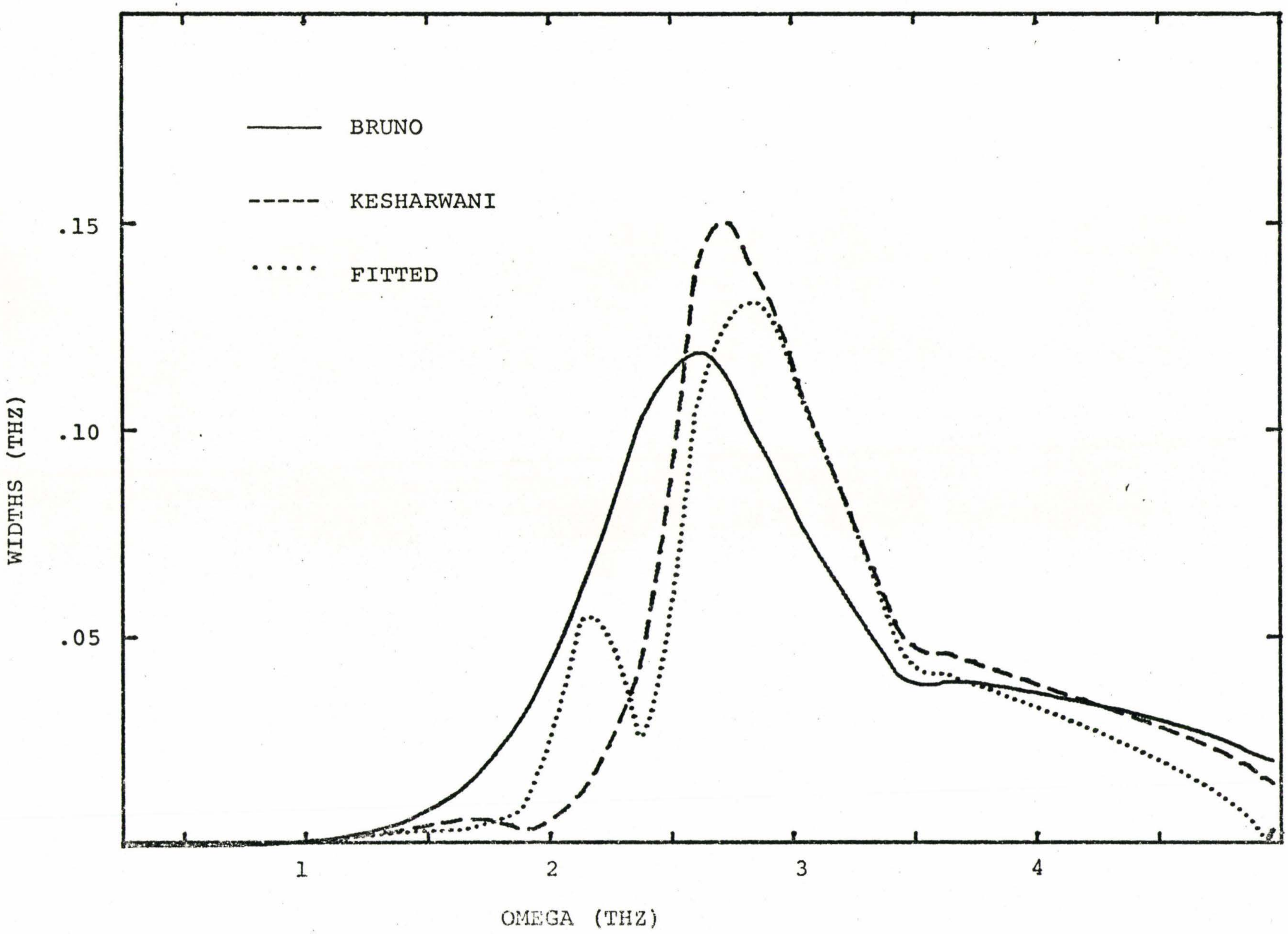

FIGURE 15

HALF-WIDTHS AT HALF-MAXIMUM IN T(zzz) DIRECTION (NO RESOLUTION EFFECT)

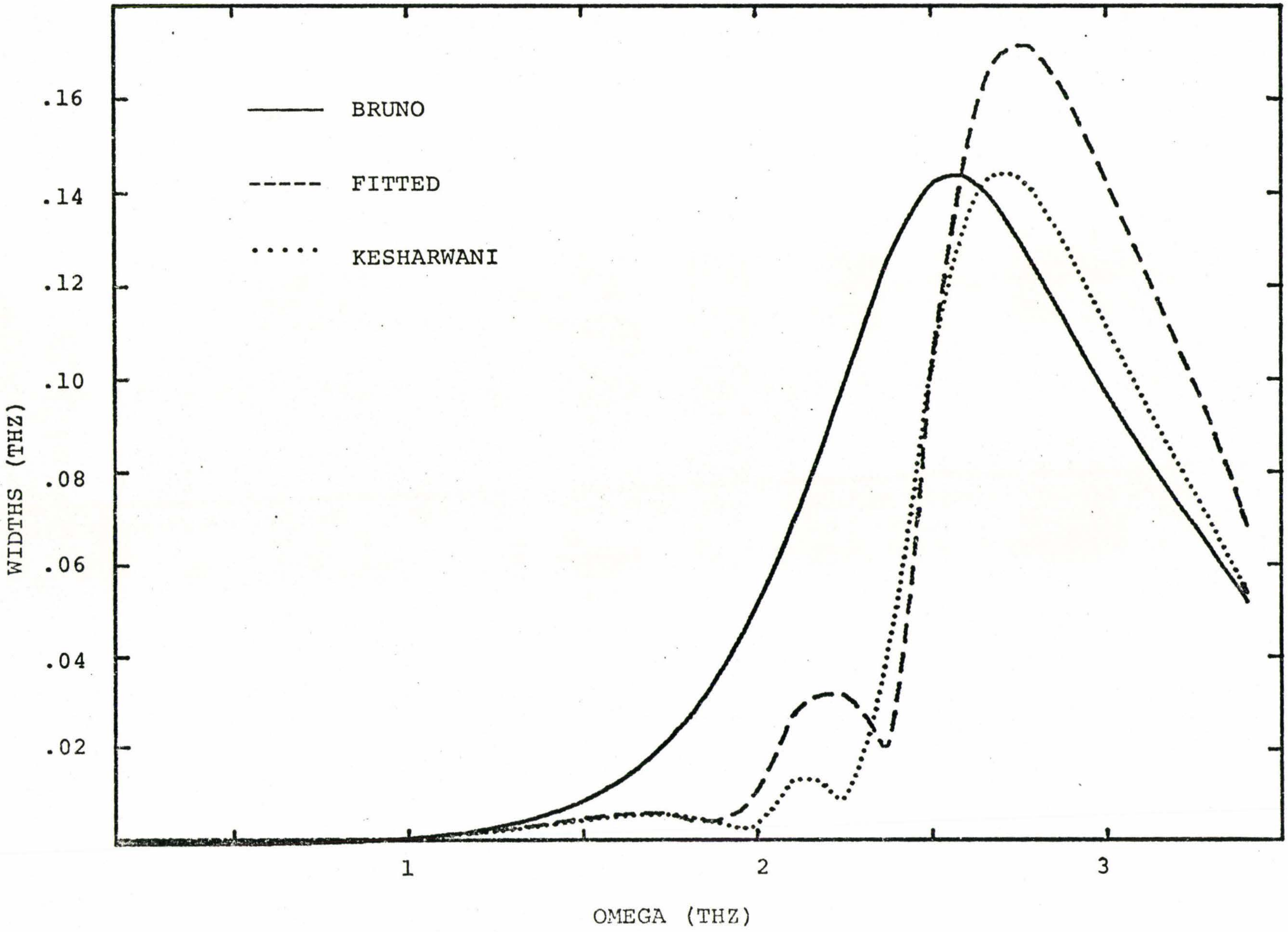

FIGURE 16

HALF-WIDTHS AT HALF-MAXIMUM IN T1(zz0) DIRECTION (NO RESOLUTION EFFECT)

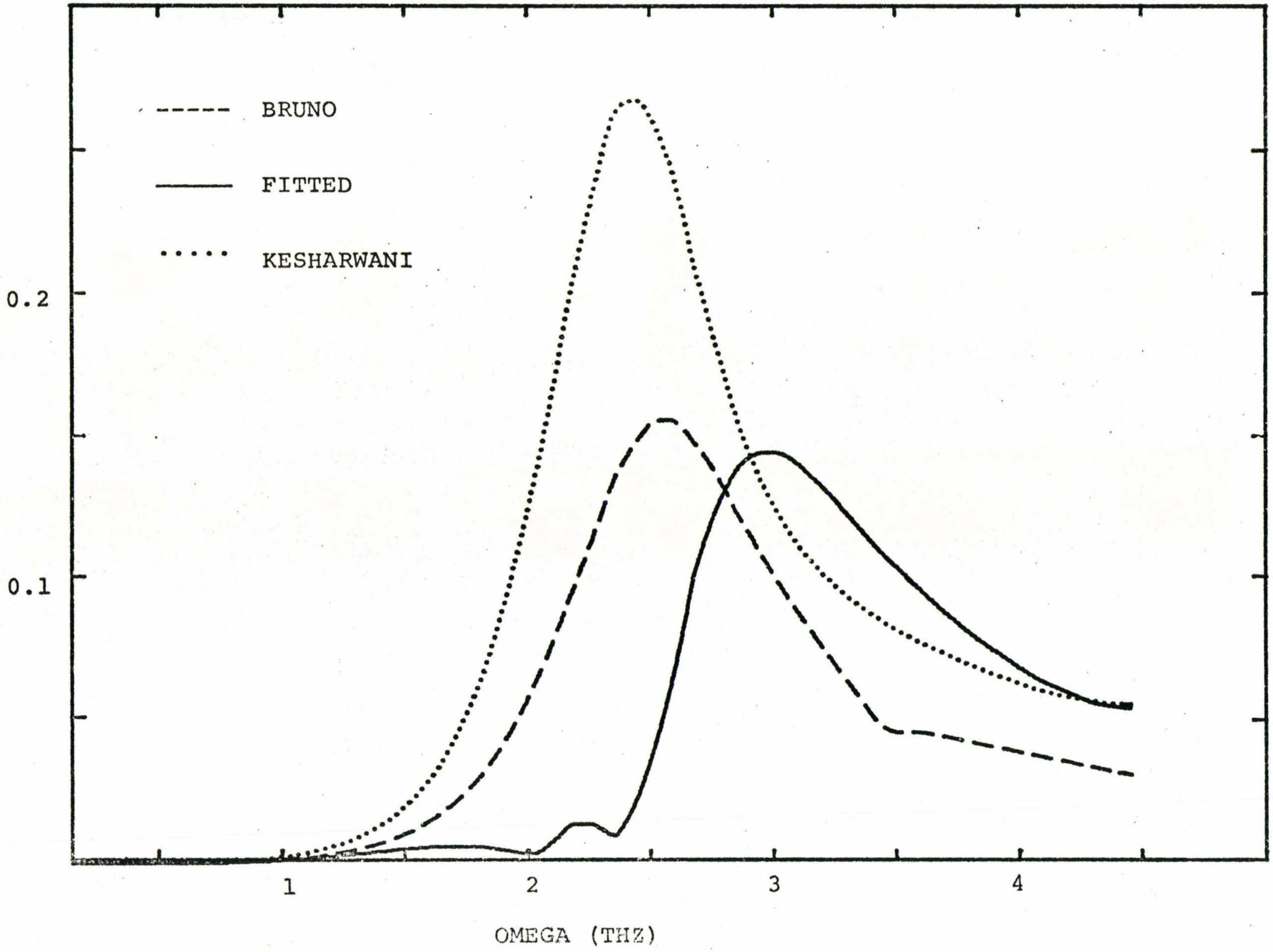

directions using his calculated Gruneisen parameters, it would seem to follow that the shifts due to the fitted changes could only be made to fit the high frequency experiments by using some rather fortuitous combinations of k-dependent Gruneisen parameters. It appears that forcing the fit at this low frequency end has distorted the results in the high frequency range, indicating that the two-parameter model is too simple to fit the results over the entire frequency range. Referring back to Table 5 we see that changing the Δ1XX force constant while holding Δ1ZZ constant had the effect of increasing both elastic constants, while increasing the Δ1ZZ force constant increased the C' elastic constant most significantly while hardly affecting the C_{44} elastic constant. Thus starting from the force constants of Bruno, it was necessary to change both force constants in opposite directions, in order to affect the change in the elastic constants, and as a result the large force constant changes have produced the distortion in the shifts at high ω.

Although Kesharwani has not shown any calculations of shifts without volume effect in his paper (1973), it is obvious that the shifts calculated here using his changes are somewhat larger than what he has shown even without the volume effect. In fact, the discrepancy amounts to as much 60% in the T(z00) direction. On the other hand, the shifts and widths calculated using the changes of Bruno and Taylor agree precisely with their results, which tends to support the validity of these calculations.

The comparison with experimental measurements of Kamitakahara (1973) in the T(zzz) branch is shown in Figs. 17 and 18. Figure 17 shows the shifts after including the effect of the overall volume change using the mode Gruneisen parameters defined by (II-18). Both Bruno and Taylor (1971) and Kesharwani and Agrawal (1973) include a calculation of the mode Gruneisen parameters in their respective papers, and it is these parameters which have been used. The widths shown in Fig. 18 include the effects of the experimental resolution. This has been done by folding the cross section function with a Gaussian, i.e.:

$$J_b(j,\underline{q},\omega) = \int \exp[-(\frac{\omega - \omega'}{2W(\underline{q})})^2] J(j,\underline{q},\omega')d\omega'$$

where

$$J(j,\underline{q},\omega) = \frac{k'}{k}\frac{e^{\beta\omega}}{e^{\beta\omega}-1} \text{Im } \tilde{G}_j(\underline{q},\omega) \quad .$$

The value of $W(\underline{q})$ is obtained by observing the widths of the pure Cu groups in this direction. The shifts and widths for the alloy are then measured offshell using $J_b(j,\underline{q},\omega)$. Kamitakahara has given the following values for these Cu widths in the T(zzz) branch:

FIGURE 17

COMPARISON OF EXPERIMENTAL AND CALCULATED SHIFTS (WITH VOLUME EFFECT) T(zzz)

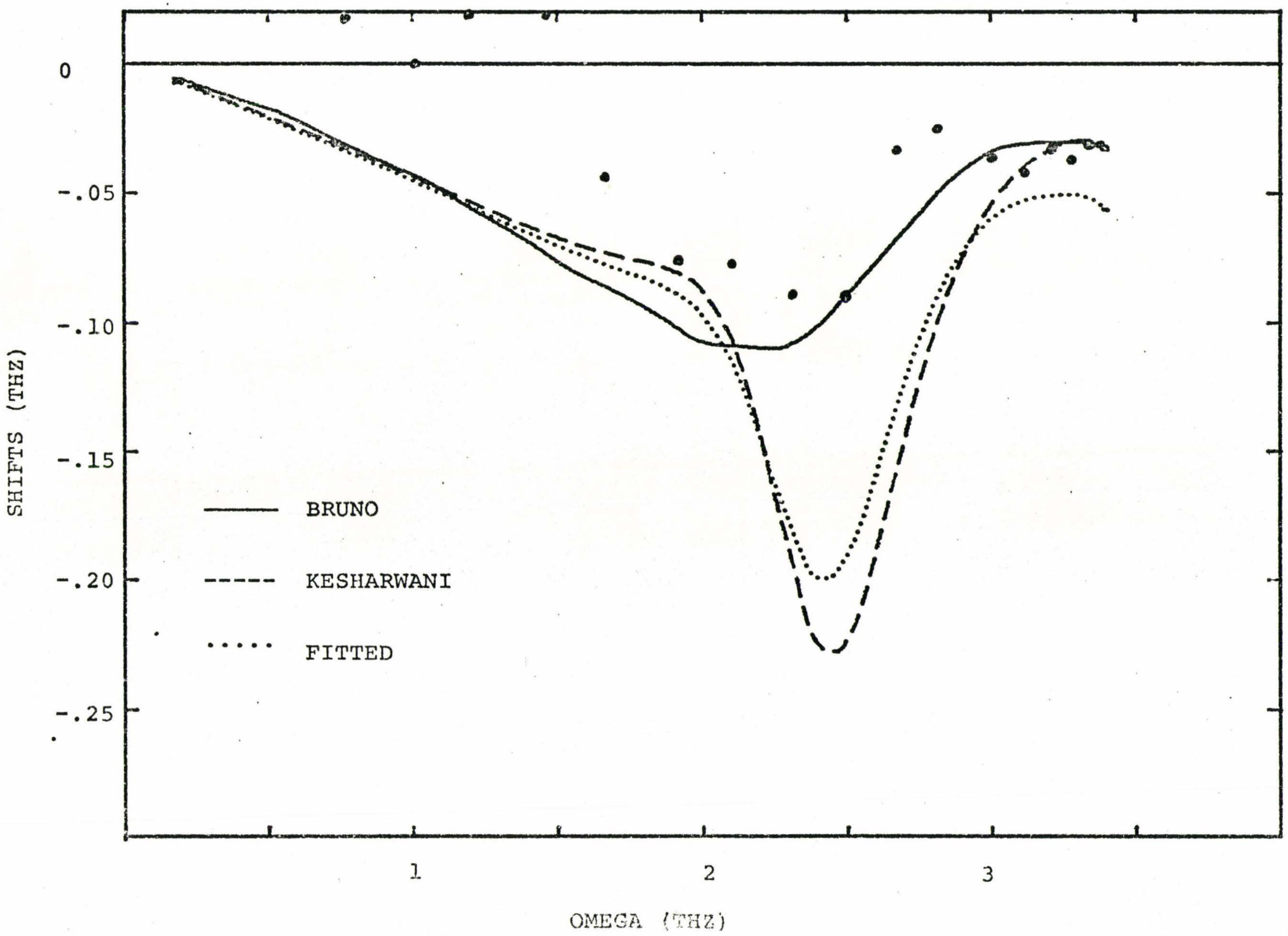

FIGURE 18

COMPARISON OF EXPERIMENTAL AND CALCULATED WIDTHS T(zzz) (BRUNO)

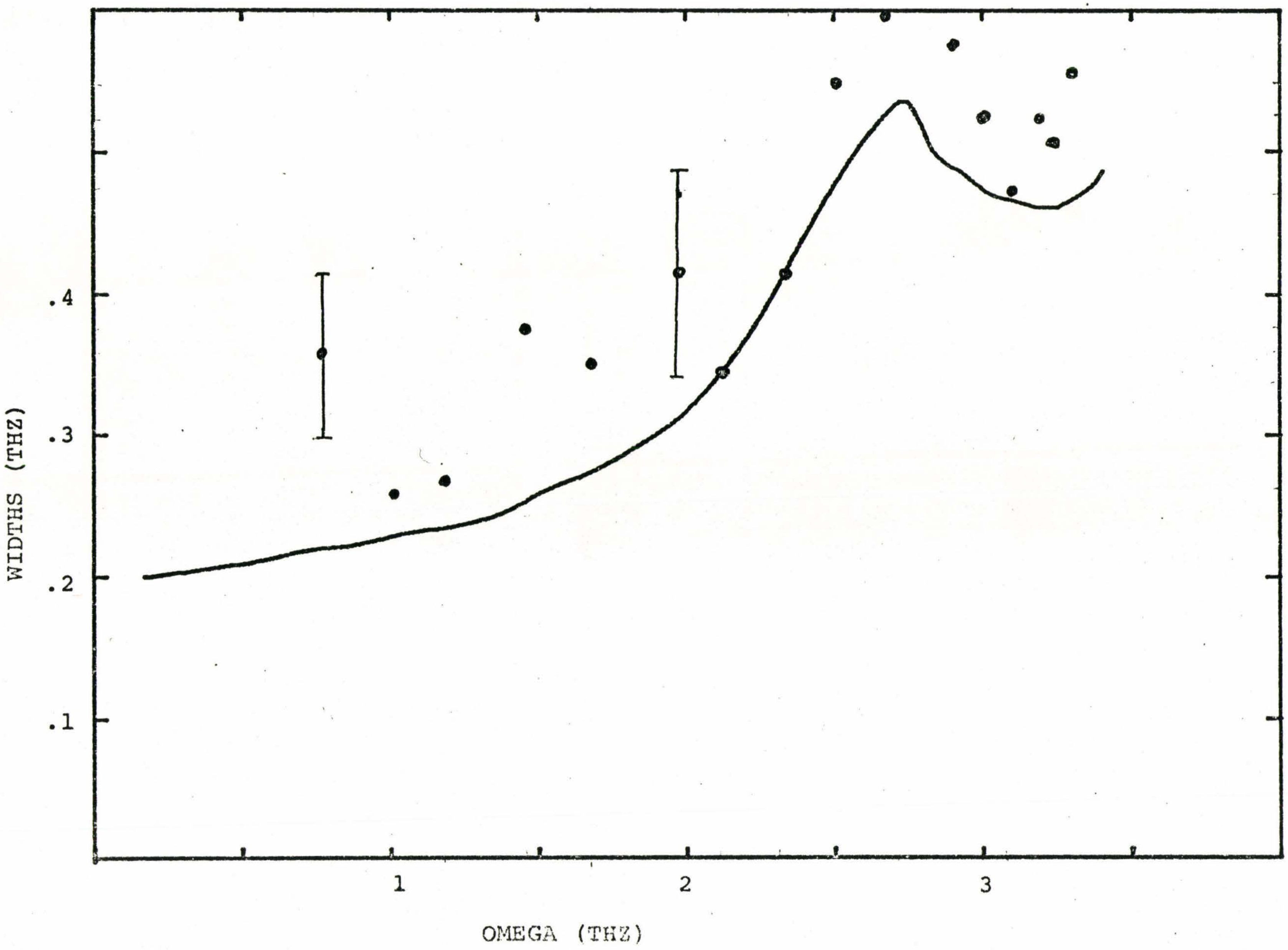

z	WIDTH(FWHM)-THZ
0.1	0.21
0.2	0.29
0.3	0.29
0.4	0.39
0.5	0.44

so that $W(\underline{q})$ is an approximately linear function chosen to give these widths.

It is obvious from both Figs. 17 and 18 that the shifts and widths calculated with Bruno's force constant changes follow the general shape of the experimental curves, but are still rather far off. In the case of the shifts, the calculations are consistently too low at low ω, but the positive shifts measured in this region would seem to cast doubt on these results. The calculated widths are too low over the entire frequency range which might indicate that the effects of the resolution have not been properly considered. As far as the shifts are concerned, it is difficult to pinpoint any one cause of error since so many approximations have been introduced to handle the change in volume of the crystal. In particular, the mode Gruneisen parameters are crucial in determining the shifts, especially such k-dependent parameters as those of Bruno and Taylor (1971).

The mode Gruneisen parameters of Kesharwani and Agrawal (1973) have been added to the shifts due to the force constant changes of Kesharwani as well as the fitted changes and are compared with experiment in Fig. 17. Here, both sets give shifts much too large in the vicinity of the resonance, but tend to follow the results of Bruno at the low frequency end. Again, it would seem that the rather large force constant changes involved have distorted the curves at the resonance.

2.5 Conclusions

It has been shown that the force constant changes fitted to the elastic constant data were unable to calculate the shifts and widths properly throughout the high frequency range, while the force constant changes adequate for the high frequency range failed to calculate the low frequency result. The obvious conclusion is that the model is too simple to cover the entire range. A more realistic calculation has to include the possibility of long-range changes, and certainly non-central volume-dependent effects should be included as is now known to be necessary for any calculations in metals. At any rate, a model with several more parameters seems essential to fit shifts and widths in all directions. Furthermore, as has been pointed out by several investigators (e.g., Kesharwani and Agrawal (1973)), the effects of the change in volume must certainly be included in a more systematic manner than has been done in these calculations, or in fact, any calculation to date. Especially in calculating the shifts, the mode Gruneisen parameters play a crucial part, and must be calculated from some realistic model. At the low frequency end, the mode Gruneisen's are known experimentally so that the elastic constant data should provide some means of fitting the force constant changes which bypasses this volume problem. However, as there are only three elastic constants, the fit will be unambiguous only for simple models, which seem to be inadequate from these calculations.

The force constant changes of Bruno and Taylor (1971) fitted to the T(z00) and Tl(zz0) branches have been shown to follow in general the trend of the experimental shifts and widths in the T(zzz) branch while deviating in some systematic manner from these results especially in the case of the widths. This seems to indicate that a more careful consideration of the effect of experimental resolution is in order, and of course, a more realistic calculation of the mode Gruneisen parameters in this direction.

The shifts and widths calculated by Kesharwani and Agrawal (1973) have not been reproduced in these calculations which indicates that there must be an error someplace. Possibly, the perturbation theory has broken down in the presence of such large force constant changes, and a comparison with the full t-matrix calculation is necessary. On the other hand, the results of Bruno and Taylor (1971) have been reproduced for all directions, and the effects of the changes in force constant changes on the shifts and widths seems to support the trends predicted by both Bruno and Taylor (1971) and Kesharwani and Agrawal (1973). The discrepancy can be resolved only by further calculations using the full t-matrix.

APPENDIX I

CRYSTAL SYMMETRY AND PERTURBATION THEORY

The point group of a crystal is the set of proper and improper rotations which take the crystal into itself. Each element of the group may be represented by the 3×3 matrix $S_{\alpha\beta}$, such that if $\underline{x}(\ell)$ is the position of the ℓ^{th} atom in the crystal, then the operative S has the effect of moving that atom to the new position $\underline{x}$ (L)

$$x_{\alpha}(L) = \sum_{\beta} S_{\alpha\beta} x_{\beta}(\ell) \quad . \tag{AI-1}$$

Maradudin, Montroll and Weiss (1971) show that the force constant matrix Φ and the perfect crystal Green's function must transform according to:

$$\Phi_{\alpha\beta}(LL') = \sum_{\gamma\delta} S_{\alpha\gamma} S_{\beta\delta} \Phi_{\gamma\delta}(\ell\ell') \tag{AI-2}$$

and

$$P_{\alpha\beta}(LL') = \sum_{\gamma\delta} S_{\alpha\gamma} S_{\beta\delta} \phi_{\gamma\delta}(\ell\ell') \tag{AI-3}$$

where the operation S takes the atom at ℓ to the position L and that at ℓ' to position L'. In particular, if the operation S leaves both ℓ and ℓ' unmoved, then the Φ-matrix must satisfy:

$$\Phi(\ell\ell') = S\Phi(\ell\ell')\tilde{S} \tag{AI-4}$$

i.e., it must be invariant, and this can be used to limit the number of independent elements in Φ.

The symmetry properties of the F.C.C. lattice, of which copper is an example, are well known.
If there is a point defect in the crystal, then the operations of the point group must be applied in such a way as to leave the defect unmoved. Under these conditions, all matrices must transform in the same way:

$$A(LL') = SA(\ell\ell')\tilde{S} \tag{AI-5}$$

where it is assumed that the defect is at $\ell = 0$. Using the operations of the O_h group which is the point group of the F.C.C. crystal, the following general results can be shown:

$$A_{\alpha\beta}(0,0) = \delta_{\alpha\beta}A_0 \quad . \tag{AI-6}$$

For the twelve first neighbours:

$$A_{\alpha\beta}(0,\ell) = A_{\alpha\beta}(0,\ell+6) \tag{AI-7}$$

where $\ell \neq 0$, ℓ and $\ell+6$ are co-linear with the defect and on opposite sides. Furthermore, the following properties are true for all force constant matrices (Maradudin, Montroll and Weiss (1971)):

$$\Phi_{\alpha\beta}(\ell\ell') = \Phi_{\beta\alpha}(\ell'\ell) \qquad \text{(AI-8)}$$

$$\sum_{\ell'} \Phi_{\alpha\beta}(\ell\ell') = 0 \qquad \text{(AI-9)}$$

and

$$\sum_{\ell\ell'} \Phi_{\alpha\beta}(\ell\ell') = 0 \quad . \qquad \text{(AI-10)}$$

Using these properties, the defect matrix for nearest neighbour force constant changes only has the form shown in Fig. A1. Each of the matrices c_i is of dimension 3×3 as shown in Fig. A2. To calculate the self-energy x by the perturbation method (I-120), it can be seen that since

$$x^{1}_{\alpha\beta}(\ell\ell') = \frac{M\varepsilon\omega^2}{1 - (1-c)M\varepsilon\omega^2 P_0}\,\delta(\alpha\beta)\delta(\ell\ell')\delta(\ell 0) \qquad \text{(AI-11)}$$

the only elements of P required are those connecting the defect to the nearest neighbours. We can, therefore, partition P in the same way as c. Furthermore, it can be seen by inspection that the matrices P^i and c^i commute for

FIGURE A1

PARTITIONING OF DEFECT MATRIX

$$
\begin{array}{ccccccccccccc}
C1 & C2 & C3 & C4 & C5 & C6 & C7 & C2 & C3 & C4 & C5 & C6 & C7 \\
C2 & -C2 & & & & & & & & & & & \\
C3 & & -C3 & & & & & & & & & & \\
C4 & & & -C4 & & & & & & & & & \\
C5 & & & & -C5 & & & & & & & & \\
C6 & & & & & -C6 & & & & & & & \\
C7 & & & & & & -C7 & & & & & & \\
C2 & & & & & & & -C2 & & & & & \\
C3 & & & & & & & & -C3 & & & & \\
C4 & & & & & & & & & -C4 & & & \\
C5 & & & & & & & & & & -C5 & & \\
C6 & & & & & & & & & & & -C6 & \\
C7 & & & & & & & & & & & & -C7
\end{array}
$$

FIGURE A2

NEAREST NEIGHBOUR FORCE CONSTANT MATRICEW

$$C1 = -\begin{pmatrix} \alpha & \gamma & 0 \\ \gamma & \alpha & 0 \\ 0 & 0 & \beta \end{pmatrix} \qquad C4 = -\begin{pmatrix} \alpha & -\gamma & 0 \\ -\gamma & \alpha & 0 \\ 0 & 0 & \beta \end{pmatrix}$$

$$C2 = -\begin{pmatrix} \alpha & 0 & \gamma \\ 0 & \beta & 0 \\ \gamma & 0 & \alpha \end{pmatrix} \qquad C5 = -\begin{pmatrix} \beta & 0 & 0 \\ 0 & \alpha & -\gamma \\ 0 & -\gamma & \alpha \end{pmatrix}$$

$$C3 = -\begin{pmatrix} \beta & 0 & 0 \\ 0 & \alpha & \gamma \\ 0 & \gamma & \alpha \end{pmatrix} \qquad C6 = -\begin{pmatrix} \alpha & 0 & -\gamma \\ 0 & \beta & 0 \\ -\gamma & 0 & \alpha \end{pmatrix}$$

each value of i. Finally, using the symmetry of the P^i and c^i allows us to partition the X-matrix as shown in Fig. A3, where

$$X^1 = t(\omega)I + \; 1 + (1-c)t(\omega)P(0;\omega)]^2\, c1$$
$$+ 4(1-c)t(\omega) \sum_{i=2}^{7} c^iP^i[1 + P(0;\omega)(1-c)t(\omega)]$$
$$- 2(1-c)^2t^2(\omega) \sum_{i=2}^{7} c^iP^{i2} \qquad \text{(AI-12)}$$

and

$$X^i = c^i[1 + (1-c)t(\omega)P(0;\omega)] - (1-c)t(\omega)c^iP^i \quad . \qquad \text{(AI-13)}$$

$t(\omega)$ is the mass defect t-matrix:

$$t(\omega) = \frac{M\varepsilon\omega^2}{1 - (1-c)M\varepsilon\omega^2P(0;\omega)} \quad . \qquad \text{(AI-14)}$$

In terms of these partitioned matrices, the transformed self-energy, Σ, can be written:

$$\Sigma^{jj'}(\underline{k},\omega) = c \sum_{\substack{\alpha\beta \\ \ell\ell'}} U(j\underline{k},\alpha\ell)X_{\alpha\beta}(\ell\ell')U^*(j'\underline{k},\beta\ell')$$
$$= cX^1_{\alpha\alpha}\,\delta_{jj'} + 2c \sum_{\alpha\beta} \sum_{\ell=2}^{7} \{-c^{\ell}_{\alpha\beta}$$
$$+ 2\cos[\underline{k}\cdot\underline{R}(\ell)]X^{\ell}_{\alpha\beta}\}\sigma^{j}_{\alpha}(\underline{k})\sigma^{*j'}_{\beta}(\underline{k}) \quad . \qquad \text{(AI-15)}$$

FIGURE A3

PARTITIONING OF SELF-ENERGY MATRIX

$$\begin{array}{ccccccccccccc}
X1 & & & & X2-X7 & & & & & & X2-X7 & & \\
 & -C2 & & & & & & & & & & & \\
 & & -C3 & & & & & & & & & & \\
X2 & & & -C4 & & & & & & & & & \\
X7 & & & & -C5 & & & & & & & & \\
 & & & & & -C6 & & & & & & & \\
 & & & & & & -C7 & & & & & & \\
 & & & & & & & -C2 & & & & & \\
 & & & & & & & & -C3 & & & & \\
X2 & & & & & & & & & -C4 & & & \\
X7 & & & & & & & & & & -C5 & & \\
 & & & & & & & & & & & -C6 & \\
 & & & & & & & & & & & & -C7
\end{array}$$

APPENDIX II

MATRIX ELEMENTS IN THE SYMMETRY DIRECTIONS

If S is an element of the point group of the crystal, the effect of this operation on the dynamical matrix follows from the definition:

$$D_{\alpha\beta}(\underline{k}) = \sum_{\ell\ell'} \Phi_{\alpha\beta}(\ell\ell')\exp(-i\underline{k}\cdot(\underline{R}_{\ell} - \underline{R}_{\ell'})) \qquad \text{(AII-1)}$$

where $\Phi_{\alpha\beta}(\ell\ell')$ is the mass reduced force constant matrix. From Appendix I, we can write

$$D_{\alpha\beta}(\underline{k}) = \sum_{\ell\ell'} \sum_{\gamma\delta} S_{\alpha\gamma}S_{\beta\delta}\Phi_{\gamma\delta}(S^{-1}\ell, S^{-1}\ell')$$

$$\times \exp(-i\underline{k}\cdot(\underline{\ell} - \underline{\ell}')), \qquad \text{(AII-2)}$$

and using the property of the scalar product that:

$$\exp(-i\underline{k}\cdot(\underline{\ell} - \underline{\ell}')) = \exp(-iS^{-1}\underline{k}\cdot(S^{-1}\underline{\ell} - S^{-1}\underline{\ell}')) \qquad \text{(AII-3)}$$

gives finally:

$$D(\underline{k}) = SD(S^{-1}\underline{k})S^{-1} \quad . \qquad \text{(AII-4)}$$

We define the group of the wave vector $\underline{k}$ as the set of those elements of the point group which leave $\underline{k}$ invariant. Denoting this group by $G_{\underline{k}}$, its elements are those operatives $S_{\underline{k}}$ such that

$$S_{\underline{k}}\underline{k} = \underline{k} \quad . \tag{AII-5}$$

Equation (AII-4) shows then that $D(\underline{k})$ commutes with all elements of $G_{\underline{k}}$. It follows that the eigenvector $\sigma^j(\underline{k})$ must transform according to some irreducible representatives of $G_{\underline{k}}$ (Tinkham (1964)), and further if ω_j^2 is two-fold degenerate, then the two eigenvectors must transform according to the two different columns of the same two-dimensional irreducible representation.

These results can be used to show that $\Sigma^{jj'}(\underline{k},\omega)$ is diagonal in j if $\underline{k}$ is in a symmetry direction. By Eq. (I-100):

$$\begin{aligned}\Sigma^{jj'}(\underline{k}) &= \sum_{\substack{\ell\ell' \\ \alpha\beta}} \exp[i\underline{k}\cdot(\underline{R}_\ell - \underline{R}_{\ell'})]\sigma_\alpha^{j*}X_{\alpha\beta}(\ell\ell')\sigma_\beta^{j'} \\ &= \langle\sigma^j|X(\underline{k})|\sigma^{j'}\rangle \quad .\end{aligned} \tag{AII-6}$$

But it can be shown that $X(\underline{k})$ commutes with every element of the group G_k in the same way as the dynamical matrix. Hence it follows that the matrix element

$$\langle\sigma^j|X|\sigma^{j'}\rangle$$

must vanish unless σ^j and $\sigma^{j'}$ both transform according to the same column of the same irreducible representation of $G_{\underline{k}}$ (Tinkham (1964)). Now, for a general $\underline{k}$, the group $G_{\underline{k}}$ has only one element; the identity, and σ^j and $\sigma^{j'}$ automatically transform according to the identity representation, so nothing can be said in this case. However, for $\underline{k}$ in certain special directions (the symmetry directions), the group $G_{\underline{k}}$ has more than one element and the result above may be deduced. The three symmetry directions in a cubic crystal are (z,0,0), (z,z,0) and (z,z,z).

In the F.C.C. crystal, for the (z,0,0) and (z,z,z) directions the transverse modes are degenerate. These two eigenvectors must then transform according to the two columns of some two-dimensional representation of $G_{\underline{k}}$. On the other hand, the longitudinal mode must transform according to the identity representation. Hence it follows immediately that the matrix element is diagonal in $\underline{k}$ for these directions. For the (z,z,0) case all modes are non-degenerate, and it must be verified by inspection that the three eigenvectors transform according to three different one-dimensional representatives of $G_{\underline{k}}$, yielding the result that $\Sigma^{jj'}$ is diagonal in j for all three directions.

REFERENCES

Agrawal, B. K. and Ram, P. M., (1972), Phys. Rev. B 5, 3308.

Aiyer, R. N., Elliott, R. J., Krumhansl, J. A. and Leath, P. L., (1969), Phys. Rev. 181, 1006.

Bruno, R., (1971), Thesis, McMaster University (unpublished).

Bruno, R. and Taylor, D. W., (1971), Can. J. Phys. 49, 2496.

Daniels, W. B., (1965), Lattice Dynamics, Wallis, R. F., Ed., (Pergamon Press, London).

Elliott, R. J. and Taylor, D. W., (1964), Proc. Roy. Soc. 83, 189; (1967), Proc. Roy. Soc. A 296, 161.

Gilat, G. and Raubenheimer, L. J., (1966), Phys. Rev. 144, 390.

Kamitakahara, W. A., (1973), private communication.

Kesharwani, K. M. and Agrawal, B. K., (1971), Phys. Rev. B 4, 4623; (1972), Phys. Rev. B 5, 2130; (1972), Phys. Rev. B 6, 2178; (1973), Phys. Rev. B 7, 5153.

Kittel, C., (1968), Introduction to Solid State Physics, 3rd ed., (John Wiley and Sons, New York).

Klein, M. V., (1963), Phys. Rev. 131, 1506.

Krebs, K., (1965), Phys. Rev. 138, A143.

Lakatos, K., (1967), Thesis, (unpublished).

Lakatos, K. and Krumhansl, J. A., (1969), Phys. Rev. 180, 729.

Langer, J. S., (1961), J. Math. Phys. 2, 584.

Lap, M., (1951), Reviews of Mod. Phys. 23, 287.

Maradudin, A. A., (1963), Astrophysics and the Many Body Problem, (W. A. Benjamin Inc., New York).

Maradudin, A. A., Montroll, E. W. and Weiss, G. H., (1971), Solid State Physics, (Suppl. No. 3), 2nd Ed.

O'Hara, S. G. and Marshall, B. J., (1971), Phys. Rev. B 3, 4002

Overton, W. C. and Gaffney, J., (1955), Phys. Rev. 98, 973.

Svensson, E. C. and Kamitakahara, W. A., (1971), Can. J. Phys. 49, 2291.

Taylor, D. W., (1964), Thesis, (unpublished); (1967), Phys. Rev. 156, 1017.

Tinkham, M., (1964), Group Theory and Quantum Mechanics, (McGraw-Hill).

Zubarev, D. N., (1960), Sov. Phys. USP., 3, 320.